

OPENXRD: A Comprehensive Benchmark Framework for LLM/MLLM XRD Question Answering[†]

Ali Vosoughi,^{*a} Ayoub Shahnazari,^{*b} Yufeng Xi,^c Zeliang Zhang,^a Griffin Hess,^b Chenliang Xu^a and Niaz Abdolrahim^{b,c,d}

We introduce OPENXRD, a comprehensive benchmarking framework for evaluating large language models (LLMs) and multimodal LLMs (MLLMs) in crystallography question answering. The framework measures context assimilation, or how models use fixed, domain-specific supporting information during inference. The framework includes 217 expert-curated X-ray diffraction (XRD) questions covering fundamental to advanced crystallographic concepts, each evaluated under closed-book (without context) and open-book (with context) conditions, where the latter includes concise reference passages generated by GPT-4.5 and refined by crystallography experts. We benchmark 74 state-of-the-art LLMs and MLLMs, including GPT-4, GPT-5, O-series, LLaVA, LLaMA, QWEN, Mistral, and Gemini families, to quantify how different architectures and scales assimilate external knowledge. Results show that mid-sized models (7B–70B parameters) gain the most from contextual materials, while very large models often show saturation or interference and the largest relative gains appear in small and mid-sized models. Expert-reviewed materials provide significantly higher improvements than AI-generated ones even when token counts are matched, confirming that content quality, not quantity, drives performance. OPENXRD offers a reproducible diagnostic benchmark for assessing reasoning, knowledge integration, and guidance sensitivity in scientific domains, and provides a foundation for future multimodal and retrieval-augmented crystallography systems.

1 Introduction

Crystallography is the scientific discipline concerned with determining the arrangement of atoms and molecules in crystalline solids^{1–3}. This structural understanding is crucial for elucidating material properties, such as symmetry, geometry, and physical characteristics^{4,5}. This understanding is crucial for progressing materials science, especially in areas like metallurgy, pharmaceuticals, and semiconductor technology^{6–10}. Central to crystallography is X-ray diffraction (XRD), a key experimental technique that enables researchers to uncover detailed information about crystal structures by examining how X-rays interact with crystalline lattices^{11–13}.

The foundational principle of XRD is Bragg’s Law, discovered by Lawrence Bragg in 1912^{14,15}. Bragg’s law describes how the angle of a diffracted X-ray beam depends on the wavelength of the X-rays and the spacing between atoms and molecules within the material^{16,17}. Using XRD, researchers analyze crystal structures to determine important parameters such as atomic arrangements, phase composition, unit cell size, grain size, crystallinity, strain, and lattice defects^{18–23}.

Advances in the analysis of large XRD data have demonstrated that conventional deep learning approaches, such as Convolutional Neural Networks (CNNs) and Graph Neural Networks (GNNs), are powerful tools, particularly for identifying or predicting crystal parameters space group labels^{24–26}, lattice con-

stants^{27,28}, or phase compositions^{29,30}. These models achieve remarkable numerical accuracy, demonstrating their efficacy for crystal classification and structural analysis tasks.

However, despite their success in quantitative predictions, these deep-learning techniques are limited in providing interpretative and explanatory insights into the underlying physics or chemistry of XRD data^{31–33}. This lack of interpretability restricts their ability to offer meaningful explanations about the material properties or structural characteristics encoded within the diffraction data. This lack of interpretability restricts the broader application of deep-learning approaches in crystallographic research, where understanding underlying phenomena is essential^{34–36}.

In contrast, recent progress in Natural Language Processing (NLP) driven by Large Language Models (LLMs), such as GPT-based architectures, has transformed various computational domains^{37–39}. LLMs demonstrate exceptional capabilities in open-ended question answering^{40,41}, multi-step reasoning^{42,43}, domain-specific question answering^{44–46}, predicting material properties^{47–49}, and extracting information from complex datasets^{50–52}. These powerful language models can potentially bridge the interpretability gap faced by traditional deep-learning models when applied to scientific fields, including materials science and crystallography^{53–55}.

For instance, Antunes *et al.* introduced CrystaLLM, an autoregressive LLM trained on millions of Crystallographic Information Files (CIFs), which encode detailed crystallographic data, including atomic coordinates, symmetry operations, lattice parameters, and space group information, to generate plausible crystal structures from given chemical compositions, demonstrating the potential of text-based crystal structure generation⁵⁶. In addition, Johansen *et al.* introduced deCIFer, an autoregressive language model on powder XRD data to produce complete crystal structures in CIF format, attaining high match rates between generated structures and experimental diffraction profiles⁵⁷.

* These authors contributed equally to this work.

^a Dept. of Computer Science, University of Rochester, Rochester, New York 14627, USA.

^b Dept. of Mechanical Engineering, University of Rochester, Rochester, 14627, NY, USA.

^c Material Science Program, University of Rochester, Rochester, 14627, NY, USA.

^d Staff Scientist, Laboratory for Laser Energetics (LLE), University of Rochester, Rochester, 14627, NY, USA.

[†] The codes and benchmarking dataset can be accessed at

<https://github.com/niaz60/OpenXRD>.

Project webpage: <https://niaz60.github.io/OpenXRD/>.

Further extending these capabilities, Choudhary introduced DiffractGPT, a generative pretrained transformer that predicts atomic structures directly from XRD patterns, particularly when chemical information is provided⁵⁸. AtomGPT, another transformer-based model by Choudhary, effectively predicts material properties such as formation energies, electronic bandgaps, and superconducting transition temperatures with accuracy comparable to GNNs⁵⁹. Beyond generative tasks, LLMs have also been employed for scientific question-answering and knowledge retrieval in the materials domain. For example, the LLaMP framework combines an LLM with a materials database to fetch and reason over crystallographic data, reducing hallucinations and improving factual accuracy in materials science QA⁵¹.

In this study, we investigate whether providing domain-specific context generated by a stronger model, such as supporting textual material, can significantly enhance the performance of weaker models or alternative configurations of the same model on specialized XRD-related questions. To rigorously test this hypothesis, we constructed a carefully selected dataset consisting of 217 multiple-choice XRD questions, each reviewed and approved by a domain expert at the Ph.D. level. Each question has only one correct answer among four provided choices, covering a range of topics from fundamental principles to complex scenarios, including issues such as basic structural geometry, unit cell dimensions, and coordination environments, to more complex concepts, including fundamental equations and symmetry analysis. Initially, we evaluate the performance of various Large LLMs, including GPT-4.5, GPT-4, O1, O3, and so forth, under closed-book conditions, where models rely solely on their pretrained internal knowledge without external assistance. Our initial results show that GPT-4.5 clearly outperforms other tested models. Based on this outcome, we employ GPT-4.5 to generate approximately one-page textual summaries. These summaries intentionally avoid explicitly stating correct answers yet offer adequate context and guidance to facilitate correct reasoning. We then reassess the performance of the other models under open-book conditions to quantify the improvement when provided with these contextual summaries, aiming to quantify the improvement enabled by this supplementary textual material.

It is important to clarify that OPENXRD is a context-assimilation benchmark rather than a retrieval system, and as such is complementary to Retrieval-Augmented Generation (RAG) rather than competing with it. While RAG is a deployment architecture that couples a retriever with a generator to fetch answer-bearing passages from large corpora at inference time, OPENXRD deliberately removes the retrieval confound by providing fixed, curated, answer-guiding passages that avoid revealing correct answers. Accordingly, our open-book setting should be interpreted as an oracle (“Gold-Standard”) RAG condition: the generator receives perfectly relevant, expert-verified context (i.e., perfect retrieval), so the measured accuracy is an upper bound on what an end-to-end RAG system could achieve with the same base model under ideal retrieval. This design isolates the language model’s ability to integrate external guidance from confounding factors such as retrieval quality, chunking, and ranking. OPENXRD does not perform retrieval and does not aspire to be

a deployable QA system; instead, it provides a controlled, reproducible setting to disclose how language models react to guidance—when it helps, when it distracts, and how sensitivity varies with model family, token budget, and content quality. These are properties that end-to-end RAG often obscures because retrieved passages can directly contain the answer. The same evaluation harness can benchmark RAG systems by replacing our oracle helper passages with retrieved chunks from a crystallography corpus, thereby decomposing end-to-end RAG accuracy into retrieval quality and language model assimilation capability. Thus, OPENXRD serves as a diagnostic complement for RAG research, not a competing alternative.

2 Methods

2.1 Dataset Selection and Curation

To evaluate language model performance in crystallography, we curated a domain-specific multiple-choice question-answering dataset comprising 217 expert-reviewed items focused exclusively on X-ray diffraction and crystallographic reasoning. To construct this dataset, we partially drew on content from Cullity’s Introduction to X-ray Diffraction¹¹. Each question includes a concise prompt, three to four answer options, a single correct answer, a brief explanation providing the scientific rationale, and an associated subtask label that enables fine-grained performance analysis across different crystallographic domains. The dataset encompasses 81 distinct crystallographic subtasks, covering a broad span of domain knowledge including crystal structure fundamentals, diffraction geometry, reciprocal-space concepts, Bragg-law applications, peak indexing, space-group interpretation, unit-cell analysis, scattering physics, microstructure effects, and additional specialized topics (see Figure 1 and Figure 2). We adopt a multiple-choice format in this foundational benchmark because it enables unambiguous, reproducible scoring across many models, avoiding the evaluator subjectivity that arises in open-ended generation. This design choice is intended to isolate *context assimilation* effects under controlled conditions rather than to fully represent real-world crystallographic workflows. Evaluating open-ended, problem-solving tasks (e.g., short-answer explanations and multi-step derivations) is an important direction but is beyond the scope of the present benchmark and is discussed as future work.

As illustrated in Figure 2, the distribution of subtask labels highlights the diversity and complexity of the topics covered in our dataset, ranging from basic definitions to advanced structural phenomena. All questions were reviewed and validated by a domain expert to ensure scientific correctness and comprehensive coverage of essential XRD subtasks.

This annotated dataset serves three primary purposes. First, it provides a benchmarking framework for testing the capability of LLMs to comprehend and apply specialized crystallographic concepts. Second, it enables fine-grained subtask-level analysis, distinguishing model performance across different categories, ranging from fundamental definitions to complex conditions. Third, it supports a comparative study between closed-book and open-book evaluation settings, allowing us to assess the impact of sup-

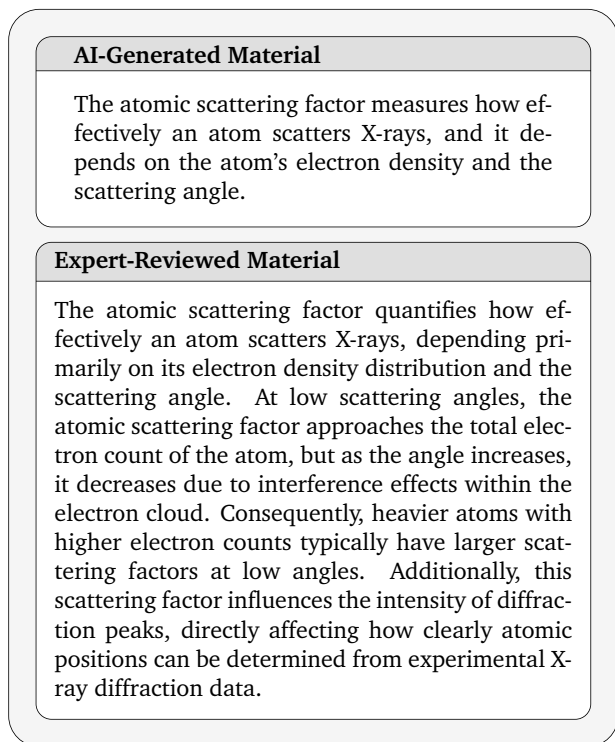


Fig. 3 The expert-reviewed version provides essential clarifications about the angular dependence of atomic scattering factors, emphasizes their direct relationship to atomic electron count, and highlights practical implications for interpreting diffraction data, elements often missed in AI-generated explanations.

maintaining concision, remove potentially misleading information, and add critical contextual details missing from the original materials.

As demonstrated in Figure 3, the expert-reviewed version provides substantial improvements over the initial AI-generated explanations. Furthermore, Figure 4 illustrates a representative example from the multiple-choice question-answering dataset, showcasing the original question, corresponding answer choices, and the AI-generated explanation as revised by an expert.

2.3.3 Quality Dimensions for Expert Review

To make expert refinement reproducible, reviewers applied four explicit quality dimensions to all 217 passages: (1) **Technical accuracy**—terminology, equations, and physical principles must be correct and precise; (2) **Conceptual precision**—the targeted mechanism must be distinguished from related but distinct phenomena to avoid distraction-based errors; (3) **Pedagogical structure**—content is organized from definitions to mechanisms to question-specific implications; (4) **Contextual relevance**—remove tangential information and focus on the knowledge gap the question targets. Reviewers kept token counts within 5% of the AI-generated versions to preserve token-matched comparisons.

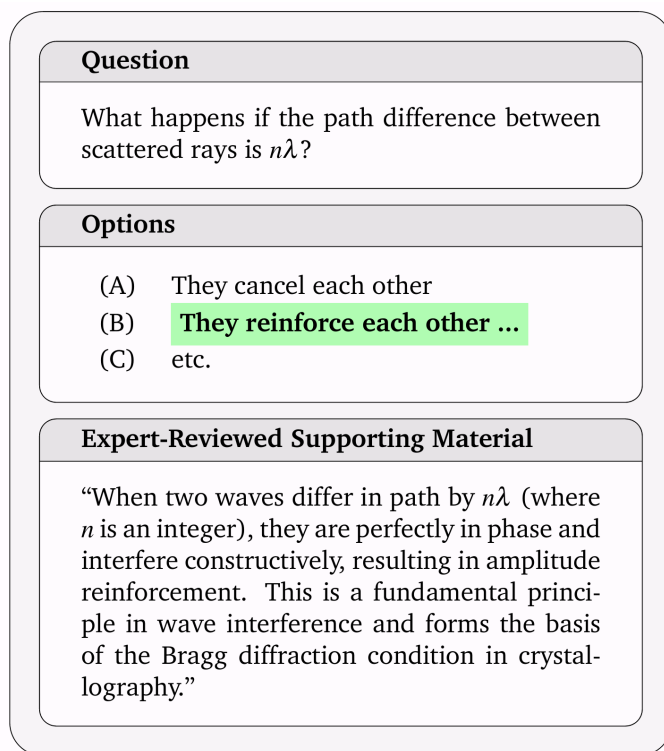


Fig. 4 An open-book mode example with expert-reviewed supporting material that clearly explains how a path difference of $n\lambda$ leads to constructive interference, with additional contextual information about its relevance to crystallography. The correct answer is highlighted in green.

2.4 Input Context Structuring

We implement a structured input preparation approach via a fusion module. For open-book evaluations, we employ a retrieve-then-read style input format (without executing retrieval) where the supporting material precedes the question:

$$x = \text{FORMAT}(x_s, x_q, x_o) \quad (1)$$

where x_s is the supporting textual content, x_q represents the question text, and x_o indicates the provided answer choices. The `FORMAT` function organizes these components with clear delimiters and instructional guidance. For closed-book evaluations, the supporting material is omitted ($x_s = \emptyset$), while the remaining formatting is preserved. This structured approach aligns with established retrieval-augmented generation paradigms, wherein external knowledge serves as contextual reference material. Here, x_s is an oracle helper passage selected and refined offline; no retriever, corpus chunking, or ranking is used in OPENXRD. Figure 5 demonstrates the architecture of this open-book QA pipeline. Currently, our implementation is exclusively textual; however, this framework can be extended to multimodal data (such as XRD patterns and crystallographic diagrams) as generative vision models become sufficiently advanced.

2.5 Evaluation Metrics

We use several metrics to quantitatively assess model performance across evaluation modes, primarily focusing on accuracy,

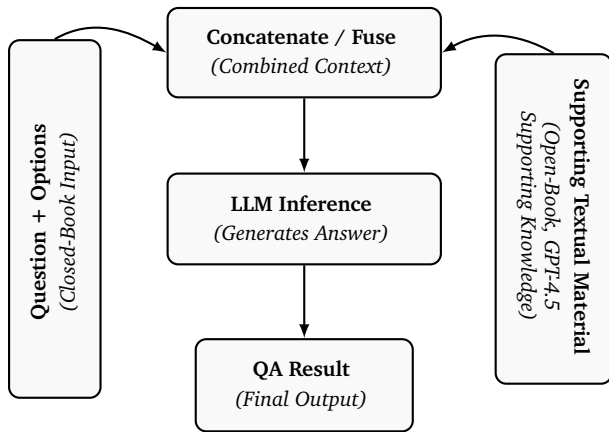


Fig. 5 Illustration of our open-book QA pipeline for crystallography. In closed-book mode, the model sees only the question (left rotated box). In open-book mode, it also receives domain-specific supporting textual material (right rotated box), which is concatenated and fed to the LLM (center pipeline), producing the final QA result.

calculated as:

$$\text{Accuracy} = \frac{|\{\text{correctly answered questions}\}|}{|\{\text{all questions}\}|} \times 100\% \quad (2)$$

For our 217-question benchmark, accuracy is reported both as an aggregated measure across the entire dataset and as a disaggregated measure by specific subtasks. For each model M and subtask $t \in \mathcal{T}$, accuracy is computed as:

$$\text{Accuracy}_{M,t} = \frac{|\{q \in \mathcal{Q}_t : M(q) = y_q\}|}{|\mathcal{Q}_t|} \times 100\% \quad (3)$$

where \mathcal{Q}_t is the set of questions associated with subtask t , y_q is the correct answer, and $M(q)$ denotes the model’s prediction. To assess the efficacy of open-book augmentation, we measure performance improvement Δ as:

$$\Delta_M = \text{Accuracy}_M^{\text{Open-Book}} - \text{Accuracy}_M^{\text{Closed-Book}} \quad (4)$$

Additionally, we quantify the relative improvement gained through expert-reviewed materials compared to AI-generated supporting materials:

$$\Delta_M^{\text{Expert}} = \text{Accuracy}_M^{\text{Open-Book, Expert}} - \text{Accuracy}_M^{\text{Open-Book, AI}} \quad (5)$$

This comprehensive evaluation framework allows us to explore several aspects. We examine the intrinsic crystallographic knowledge inherent in each model, referred to as closed-book performance. We also assess each model’s ability to leverage external knowledge effectively, known as open-book improvement. Additionally, we evaluate the added value provided by expert-reviewed supporting materials, termed expert refinement differential. Furthermore, we analyze model-specific strengths and weaknesses across various crystallographic subtasks.

2.6 Benchmark Reproducibility and Extension Guidelines

To establish OPENXRD as a reliable community benchmark with reproducible content standards, we provide documentation and

tools for three primary use cases.

Public release. All benchmark materials are publicly available at <https://github.com/niaz60/OpenXRD> and will be archived on Zenodo with DOI upon acceptance. The release includes: full question set with answers and explanations; AI-generated and expert-reviewed supporting passages for all 217 questions; GPT-4.5 generation prompts with parameters; expert-review guidelines with the four-dimension quality rubric; token matching scripts; and validation protocols for answer-guidance testing.

Evaluating new models. Researchers should download the full benchmark, run the closed-book and open-book protocols (AI and expert passages) using our scripts, and compare against baseline tables to contextualize results.

Creating new crystallography questions. Follow our question template (prompt, 3–4 options, single correct answer, brief explanation, subtask label); generate initial passages with our GPT-4.5 prompt template (“Given question... provide a concise explanation... Target 500–600 tokens”); regenerate any passage that reveals the answer or has technical errors; apply expert review using the four dimensions; token-match AI and expert versions to <5% difference ($r > 0.90$).

Domain adaptation. For new scientific domains, adapt the generation prompt to domain terminology, recruit domain experts to review using the same four dimensions, validate answer-guidance properties on held-out models, and document domain-specific modifications.

Validation protocol. To ensure supporting materials are answer-guiding without being answer-revealing: (1) choose 3–5 held-out models across capacity tiers; (2) test on 20–30 questions in three conditions—closed-book, explicit-answer materials, candidate materials; (3) candidate materials pass if performance lies between closed-book and explicit-answer conditions and preserves the closed-book model ranking. This confirms that materials aid reasoning without providing shortcuts.

2.7 Context Assimilation vs. Parameter Fine-Tuning

OPENXRD evaluates *context assimilation*—how models utilize short, answer-guiding passages provided at inference time. We intentionally do not modify model weights through parameter-efficient fine-tuning (PEFT) methods such as LoRA⁶⁰, as this would target a fundamentally different research question: parametric knowledge embedding rather than inference-time guidance utilization. Throughout this work, expert refinement refers to refinement of the supporting passages, not to any modification of evaluated LLMs. Accordingly, any performance changes in open-book mode should be interpreted as improved use of provided context (context assimilation), not weight-level refinement of model reasoning.

Several factors motivate this scope decision. First, many of the 74 models in our evaluation pool are API-only or closed-weight systems (GPT-4.5, O3-mini, Claude variants) that cannot be fine-tuned uniformly, making fair PEFT comparisons intractable. Second, our 217-question benchmark is intentionally reserved as a held-out evaluation set to preserve benchmark integrity; fine-tuning on these questions or near-duplicates would

introduce data leakage and undermine reproducibility. Third, PEFT optimization conflates parametric adaptation effects with the inference-time assimilation dynamics we aim to isolate.

OPENXRD is complementary to PEFT research rather than competitive with it. Researchers can fine-tune open-weight models on external crystallographic corpora and subsequently use OPENXRD to test whether inference-time guidance remains beneficial, becomes redundant, or introduces interference after domain adaptation. This decomposition of parametric knowledge versus contextual reasoning is precisely the diagnostic capability OPENXRD provides. For researchers aiming to perform PEFT studies using our benchmark, we provide the complete dataset, evaluation scripts, and code framework on our project repository. This open-source release enables researchers to design their own PEFT experiments using standard techniques such as LoRA with appropriate data splits to prevent leakage between training and evaluation sets.

3 Results

In this section, we present a detailed evaluation of our OPENXRD benchmark for crystallography, using a curated set of 217 XRD-related questions. Each question can be answered in two ways: Closed-book mode, where the model relies solely on its internal knowledge, and Open-book mode, where it consults supporting textual material. Our goal is to determine to what extent supporting textual material access bolsters model performance, particularly for advanced domain-specific queries. We conduct our experiments in two phases: first using AI-generated supporting materials provided by GPT-4.5, and then using expert-reviewed versions of these materials to assess whether human domain expertise further enhances performance.

3.1 Setup and Baselines

3.1.1 Models Compared

We conduct a comprehensive evaluation across 74 state-of-the-art language models and vision-language models spanning multiple architectural families, parameter scales, and specialization domains. This extensive model selection enables systematic analysis of how model architecture, scale, and domain adaptation affect crystallographic reasoning performance under both closed-book and open-book conditions.

OpenAI models. We evaluate 13 OpenAI models across multiple generations and capabilities. The next-generation GPT-5 series includes `gpt-5` and `gpt-5-codex`^{61,62}. The reasoning-optimized O-series comprises `o3-mini` (`o3-mini-2025-01-31`), `o1` (`o1-2024-12-17`), and `o1-mini`^{63,64}. The GPT-4 family includes `gpt-4.5-preview` (`gpt-4.5-preview-2025-02-27`), `gpt-4o`, `gpt-4o-mini`, `gpt-4-turbo` (`gpt-4-turbo-2024-04-09`), `gpt-4-turbo-preview` (`gpt-4-preview-0125`), `gpt-4-0314` (`gpt-4-0613`), and the base `gpt-4`⁶⁵⁻⁶⁸. We also evaluate earlier-generation models `gpt-3.5-turbo` and `gpt-3.5-turbo-16k`^{69,70}. *Anthropic Claude models.* We assess four Claude variants spanning two generations: `claude-3.5-sonnet`, `claude-3.5-haiku`, `claude-3-opus`, and `claude-3-haiku`⁷¹⁻⁷³. *Meta LLaMA*

models. The LLaMA family is represented by six models across three generations and multiple parameter scales: `llama-3.1-405b-instruct` (405B parameters), `llama-3.1-70b-instruct` and `llama-3-70b-instruct` (70B parameters), `llama-3.1-8b-instruct` and `llama-3-8b-instruct` (8B parameters), and `llama-3.2-3b-instruct` (3B parameters)^{74,75}.

QWEN/Alibaba models. We evaluate 10 models from Alibaba’s QWEN ecosystem. General-purpose models include `qwen3-next-80b-a3b-instruct`, `qwen3-next-80b-a3b-thinking` (reasoning-optimized variant), `qwen-2.5-72b-instruct`, `qwen-plus`, `qwen-max`, and `qwen-2.5-7b-instruct`^{76,77}. Code-specialized variants include `qwen3-coder-flash`, `qwen3-coder-plus`, and `qwen-2.5-coder-32b-instruct`^{78,79}. We also evaluate `tongyi-deepresearch-30b-a3b`, Alibaba’s research-focused model⁸⁰. *Mistral AI models.* Seven Mistral variants are evaluated: `mistral-large` and `mistral-small` (dense models)^{81,82}, `mistral-7b-instruct` and `mistral-7b-instruct-v0.1` (7B base models)⁸³, the mixture-of-experts models `mixtral-8x22b-instruct` and `mixtral-8x7b-instruct`^{84,85}, and the multimodal `pixtral-12b`⁸⁶. *DeepSeek models.* We evaluate two DeepSeek variants: `deepseek-v3.1-terminus` and `deepseek-chat`⁸⁷. *Google models.* Three Google models are assessed: the flagship `gemini-2.5-pro` and the open-weight models `gemma-2-27b-it` and `gemma-2-9b-it`^{88,89}. *Amazon Nova models.* We evaluate Amazon’s Nova series across three capability tiers: `nova-pro-v1`, `nova-lite-v1`, and `nova-micro-v1`⁹⁰. *X.AI models.* We include X.AI’s `grok-4-fast` in our evaluation⁹¹. *LLaVA vision-language models.* Ten LLaVA variants are evaluated, spanning multiple generations and backbone architectures. These include `llava-v1.6-34b` and `llava-v1.6-mistral-7b` from the 1.6 series⁹², `llava-v1.5-13b` and `llava-v1.5-7b` from the 1.5 series⁹³, and six LLaVA-OneVision models with QWEN2 backbones: `llava-onevision-qwen2-7b-si`, `llava-onevision-qwen2-7b-ov-chat`, `llava-onevision-qwen2-7b-ov` (7B variants), and `llava-onevision-qwen2-0.5b-ov`, `llava-onevision-qwen2-0.5b-si` (0.5B variants)⁹⁴. These models combine vision encoders (ViT) with LLM backbones (Mistral, LLaMA, QWEN) for multimodal understanding. In our text-only evaluation setting, these models process supporting textual materials that may include image captions but not the actual images themselves. *LLaMAT crystallography-specialized models:* We evaluate three domain-adapted LLaMAT variants that have been pre-trained on crystallographic information files (CIF): `llamat-3-chat`, `llamat-2-chat`, and `llamat-2`⁹⁵. These models represent explicit attempts to enhance materials science reasoning through domain-specific pre-training.

Dziner models. We assess three Dziner-QWEN variants spanning different parameter scales: `dziner-qwen-2.5-72b`, `dziner-qwen-2.5-coder-32b`, and `dziner-qwen-2.5-7b`⁹⁶.

Perplexity models. Two Perplexity variants are evaluated: `sonar-pro` and `sonar`^{97,98}. *Additional specialized models.* Our evaluation includes several community-developed and specialized models: Meituan’s

longcat-flash-chat⁹⁹, Arcee-AI’s afm-4.5b¹⁰⁰, the community-tuned models undi95/remm-slerp-12-13b and gryphe/mythomax-12-13b^{101,102}, the vision-language models honeybee-13b and honeybee-7b¹⁰³, and the routing system openrouter/auto¹⁰⁴.

This comprehensive model selection, spanning from 0.5B to 405B+ parameters and covering generalist, reasoning-optimized, code-specialized, domain-adapted, and vision-language architectures, enables robust analysis of how different model capabilities interact with domain-specific supporting materials in crystallographic question answering.

Several models were considered but ultimately excluded from our evaluation due to architectural incompatibilities or technical limitations. The *Ether-0* model¹⁰⁵, designed specifically as a reward model for scoring the quality of scientific reasoning in chemistry rather than as a generative question-answering system, was deemed inappropriate for our benchmark. Reward models are trained using preference learning objectives to rank or score candidate responses, fundamentally differing from generative models that produce answers directly. This architectural mismatch makes *Ether-0* incompatible with our multiple-choice QA evaluation framework, which requires models to generate or select answers rather than evaluate them.

We also encountered technical challenges with several LLaMAT variants—specialized adaptations of LLaMA models pre-trained on crystallographic information files (CIF). While three LLaMAT models (*llamat-3-chat*, *llamat-2-chat*, and *llamat-2*) were successfully evaluated after configuring `max_model_len=2048` to accommodate their tokenization schemes, three additional variants (*llamat-3-base*, *llamat-3-cif*, and *llamat-2-cif*) exhibited incomplete HuggingFace configurations: the base *llamat-3* model lacked proper architecture specifications in `config.json`, while both CIF-specialized variants had malformed model cards with missing tokenizer bindings that prevented inference initialization. Given that the successfully evaluated chat-optimized LLaMAT variants achieved moderate baseline performance (50.69-57.14% accuracy in closed-book mode; see Table 2), the exclusion of these broken variants does not materially impact our conclusions about crystallography-specialized models.

To facilitate systematic performance analysis across different capability levels, we categorize the 74 evaluated models into three size groups based on parameter count and architectural complexity, as summarized in Table 1. This categorization enables structured comparison of how model scale affects the ability to assimilate external domain knowledge in crystallography tasks.

Table 1 Model categorization by size for systematic performance analysis. The 74 evaluated models are grouped into three categories to examine scale-dependent effects on external knowledge assimilation in crystallography.

Category	Size Range	Representative Models
Small models	< 10B parameters	Mistral-7B, Phi-3-Mini (3.8B), Llama-3-8B, LLaVA-v1.5-7B, QWEN2-0.5B, HoneyBee-7B, LLaMAT-2 (7B), AFM-4.5B
Mid-sized models	10B–70B parameters	Llama-3-70B, LLaVA-v1.6-34B, QWEN-2.5-32B, Mixtral-8×7B (~56B active), Gemma-2-27B, Mistral-Small (24B)
Large models	> 70B parameters (or closed-weight API models)	Llama-3.1-405B, QWEN-2.5-72B, dziner-qwen-2.5-72B, GPT-4, GPT-5, GPT-4.5, O3-mini, Claude-3-Opus, Gemini-2.5-Pro, DeepSeek-V3.1

3.1.2 Inference Setup

We employ a zero-shot inference paradigm for all models without parameter updating or fine-tuning on our crystallography evaluation set. For each query, we construct a prompt consisting of the question and enumerated options, formatted consistently across all models. No in-context learning examples or demonstrations are provided, requiring models to rely entirely on their parametric knowledge. All foundation models are evaluated using their published weights and architectures; O-family models have documented parameter-efficient training on scientific corpora, while vision-language models in the LLaVA family were primarily trained on general domain text-image pairs without domain-specific adaptation to crystallography.

3.1.3 Experimental Progression

Our experimental approach follows two distinct phases: In the first phase, we use GPT-4.5 to generate supporting textual materials for each question, carefully prompting it to provide relevant information without revealing the answer. Following this, in the second phase, we engaged three Ph.D. students specializing in crystallography, with four to seven years of research experience, to review and refine the supporting materials for improved accuracy and pedagogical clarity. This two-phase approach allows us to quantify the value added by human domain expertise in the construction of supporting materials relative to state-of-the-art AI generation.

3.2 Closed-Book Mode Observations

Table 2 presents the closed-book mode accuracy achieved on our 217-question crystallography benchmark, and Figure 6 illustrates the categorized closed-book performance of the models.

O3-mini performs extremely well, achieving about 93.55% accuracy, even surpassing some GPT-4 variants, possibly reflecting training or optimization details not disclosed; we report the observed performance. However, smaller LLaVA-based models face challenges with advanced reflection extinctions, often incorrectly identifying which plane indices vanish for BCC or confusing zone-axis notation. Despite these issues, nearly all models correctly answer basic factual questions like the number of crystal systems and who discovered X-ray diffraction.

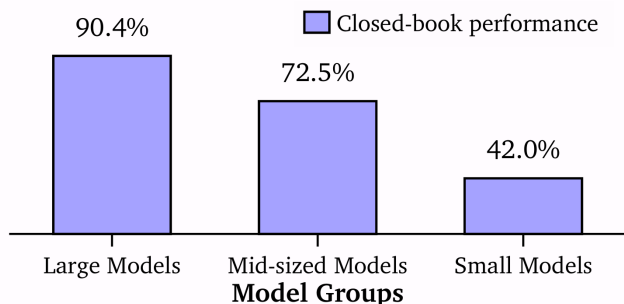


Fig. 6 Comparison of closed-book performance by model size group. Large Models (>70B parameters or advanced architectures like GPT-4, GPT-5, O1, O3-mini, n=27); Mid-sized Models (>7B-70B parameters including LLaVA-34B, QWEN2-7B, Mistral-7B, various 8B-13B models, n=22); Small Models (\leq 7B parameters including QWEN2-0.5B, LLaMA-3.2-3B, Honeybee-7B, LLaMAT-2, n=25). Analysis excludes unreliable llava-v1.6-vicuna variants.

3.3 Open-Book Mode Observations Using AI-Generated Materials (No Expert Review)

Table 3 lists the closed-book mode vs. open-book mode accuracy on our 217-question crystallography benchmark. Here and in subsequent tables, Δ represents the performance improvement defined in Equation (4), with model subscripts omitted as each row corresponds to a different model. We first evaluate open-book mode accuracy by giving each model relevant supporting textual material generated by GPT-4.5.

We observe distinct performance patterns across model scales, architectures, and domain specializations. Remarkably, specialized coder models demonstrate the most dramatic improvements: qwen3-coder-plus gains +65.95% and qwen3-coder-flash gains +40.87% from AI-generated supporting materials, suggesting these models have significant reasoning capacity but minimal crystallographic knowledge. Among general-purpose models, mid-sized architectures (>7B-70B parameters) show substantial benefits, with models like llama-3.1-8b-instruct (+6.00%), llava-onevision-qwen2-7b-ov-chat (+6.45%), anthropic/claude-3-haiku (+8.45%), and llava-v1.6-34b (+5.99%) gaining meaningfully from domain-specific context. Larger models (70B+) such as llama-3.1-405b-instruct (-4.61%), llama-3-70b-instruct (-4.14%), and qwen-2.5-72b-instruct (-1.38%) show minimal improvement or slight degradation, while very large frontier models like o3-mini see only minor gains (-4.15%), suggesting they already possess substantial internal crystallographic knowledge.

Notably, multiple frontier models show performance degradation with AI-generated supporting materials: GPT-4.5-preview (-2.31%), Claude-3.5-Sonnet (-1.84%), dziner-qwen-2.5-72b (-3.22%), and mistral-large (-2.31%). This counterintuitive pattern reveals an important failure mode: for models with comprehensive pre-trained knowledge, additional context—even when domain-relevant—can introduce interference rather than assistance.

Figure 8 shows a concrete example where supporting materials have caused confusion, directly illustrating this interference

mechanism. In this case, LLaVA-v1.6-34B answered correctly in closed-book mode (Option B: Electron cloud interference) but was misled in open-book mode to select Option C (Thermal vibration). The supporting material discussed both phenomena in close proximity: “The atomic scattering factor decreases with increasing scattering angle due to interference effects within the electron cloud. Additionally, thermal vibrations (Debye-Waller factor) can further dampen the intensity...” This juxtaposition caused the model to conflate two distinct mechanisms—the intrinsic angular dependence (correct answer) versus temperature-dependent effects (distractor)—demonstrating that the failure mode is primarily *conceptual interference* and *distraction from related concepts* rather than simple information overload or redundancy.

Our detailed analysis of the AI-generated supporting materials revealed several limitations: occasional technical inaccuracies in specialized crystallographic terminology, inadequate depth of explanation for particularly complex phenomena, information presented at times being too general to help with specific question nuances, and in some cases, the supporting materials were tangential to the precise knowledge needed for the question. Figure 7 summarizes these patterns by model size group, showing that mid-sized and small models benefit substantially from AI-generated materials (+5.3% and +10.3% respectively), while large models experience slight degradation (-1.9%).

These observations led us to hypothesize that expert-reviewed materials might yield greater performance improvements, particularly for mid-sized models with significant capacity but incomplete domain knowledge.

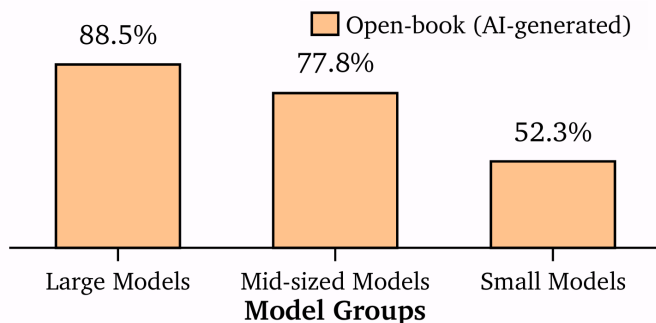


Fig. 7 Open-book performance with AI-generated supporting materials by model size group. Large Models (>70B parameters or advanced architectures, n=27); Mid-sized Models (>7B-70B parameters, n=22); Small Models (\leq 7B parameters, n=25). Compared to closed-book performance (Figure 6), large models show slight degradation (-1.9%), while mid-sized models gain +5.3% and small models gain +10.3%, demonstrating that AI-generated context benefits models with knowledge gaps but can interfere with already-capable models.

3.4 Open-Book Mode Observations Using AI-Generated Materials with Expert Review

Building on the findings from the initial open-book evaluations, we introduced expert review to improve the quality and effectiveness of the supporting materials. Three PhD-level crystallography

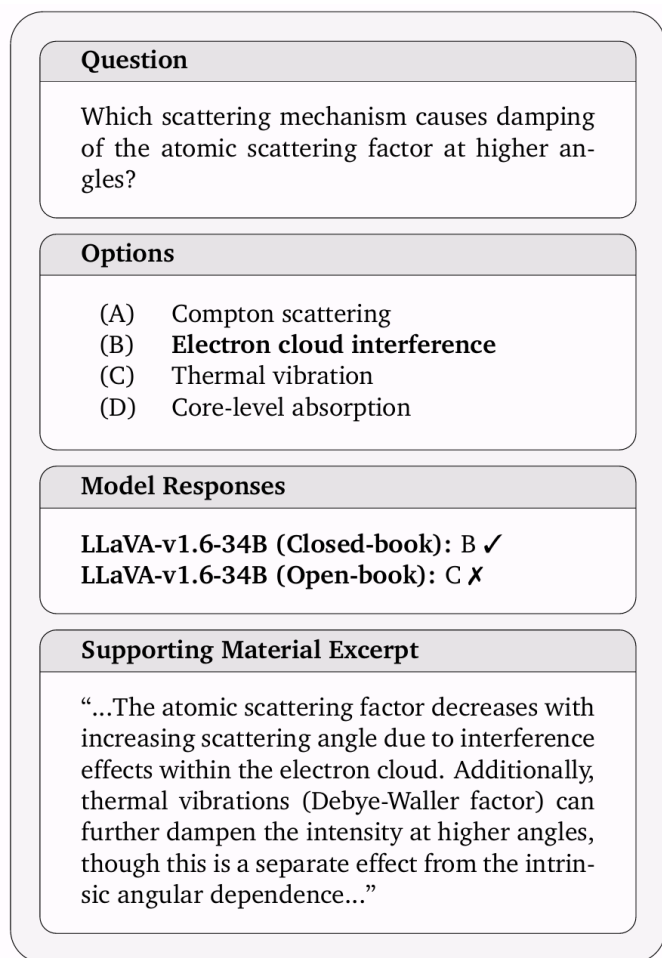


Fig. 8 Example of confusion in LLaVA-v1.6-34B due to conflicting supporting material. The model had correct knowledge in closed-book mode but was misled by additional content that mentioned both the correct answer and a distractor as possible factors affecting scattering, albeit in different ways.

experts were engaged to refine the AI-generated materials.

Table 4 compares model accuracy in closed-book and open-book modes using expert-reviewed supporting materials across our 217-question crystallography benchmark. The results show substantially improved performance, particularly among LLaVA-based models.

Remarkably, specialized coder models show the most dramatic gains, with qwen3-coder-plus (+65.95%) and qwen3-coder-flash (+42.25%) achieving exceptional improvements from very low baselines. Among more general-purpose vision-language models, the largest accuracy gains are observed in LLaVA-v1.6-34B (+11.52%) and LLaVA-v1.6-mistral-7B (+11.07%), highlighting the effectiveness of expert-curated guidance in boosting model reasoning.

Several other mid-sized models, such as LLaVA-onevision-QWEN2-7B-ov-chat (+10.14%) and LLaVA-onevision-QWEN2-7B-ov (+8.75%), also demonstrate notable improvements. Figure 9 illustrates these gains aggregated by model size group, showing that expert curation provides additional improvements over AI-generated materials, particularly for mid-sized (+1.7%)

and small models (+2.5%), while large models maintain stable performance.

A notable failure mode identified in our analysis is catastrophic degradation in domain-specialized models, which experience substantial performance drops despite receiving expert-reviewed supporting materials. As summarized in Tables 3–4, the LLaMAT family—pretrained on materials-science literature and domain-focused instruction datasets—shows the most severe declines. LLaMAT-3-chat falls from 57.14% (closed-book) to 31.80% (open-book with expert review), a –25.34% drop, while LLaMAT-2-chat decreases from 50.69% to 16.13%, a –34.56% degradation that renders the model nearly unusable in open-book mode. Only the base llama-2 model shows a modest improvement (+3.23%), though its low absolute accuracy indicates fundamental capacity limitations regardless of external support. These results demonstrate that domain specialization alone does not guarantee effective external-knowledge integration.

Similar patterns emerge in other domain-focused families. The HoneyBee models, designed primarily for scientific figure interpretation, show limited transferability to text-only crystallographic reasoning. HoneyBee-13B drops from 22.12% to 21.20% (–0.92%), and HoneyBee-7B from 19.35% to 17.51% (–1.84%), suggesting that pretraining on visual-scientific corpora does not enhance performance on purely textual tasks, and that their small parameter scale (7B–13B) restricts knowledge retention. The dZiner family, consisting of QWEN variants fine-tuned on materials-science corpora, exhibits a similar sensitivity to interference. While dZiner-QWEN-2.5-72B attains strong closed-book accuracy (90.32%), it drops to 86.18% (–4.14%) with expert-reviewed materials. The medium-sized dZiner-QWEN-2.5-coder-32B declines by –6.45%, and the smaller dZiner-QWEN-2.5-7B by –2.31%. These negative open-book effects mirror degradation trends observed in other high-capacity models, indicating that domain-specific pretraining raises baseline performance but simultaneously increases vulnerability to information interference.

Across all three families, the underlying mechanism is representational rigidity introduced during domain adaptation. These models internalize crystallographic and materials-science concepts in narrowly defined textual, visual, or instructional formats. When exposed to expert-reviewed passages that express these concepts using more pedagogical, descriptive, or stylistically diverse language, they encounter distributional mismatch between their internal priors and the external context. Even when the supplemental information is factually correct, this mismatch triggers interference rather than assistance, leading to performance degradation. This reveals a fundamental trade-off in domain specialization: while narrow, domain-focused pretraining can strengthen closed-book accuracy, it reduces flexibility in assimilating new or differently framed knowledge sources.

Interestingly, the knowledge-interference failure pattern extends systematically across top-tier models, as explained in Section 3.3. As summarized in Table 4, in the transition from the closed-book setting to the open-book mode with expert-reviewed supporting materials, several frontier systems show measurable degradation despite their high baseline accuracy. GPT-4.5-preview declines from 92.63% to 89.40% (–3.23 per-

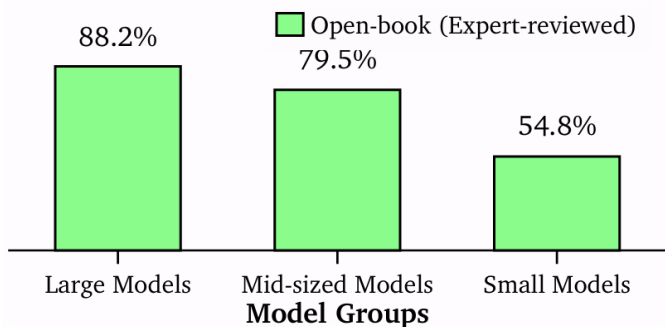


Fig. 9 Open-book performance with expert-reviewed supporting materials by model size group. Large Models ($>70B$ parameters or advanced architectures, $n=27$); Mid-sized Models ($>7B-70B$ parameters, $n=22$); Small Models ($\leq 7B$ parameters, $n=25$). Compared to AI-generated materials (Figure 7), expert curation provides additional gains for mid-sized (+1.7%) and small models (+2.5%), while large models remain stable, demonstrating that content quality improvements benefit models with reasoning capacity but incomplete domain knowledge.

centage points), while other state-of-the-art models exhibit comparable or greater decreases: openai/gpt-5 (-3.68%), x-ai/grok-4-fast (-5.78%), openai/gpt-5-codex (-4.14%), and O3-mini (-3.69%). Importantly, all of these systems exceed 90% closed-book accuracy, confirming that they already possess extensive crystallographic knowledge. The consistency of this degradation across diverse architectures (spanning distinct training paradigms, model families, and organizations) indicates that knowledge interference is an intrinsic characteristic of high-capacity language models rather than a model-specific artifact. These models appear highly sensitive to redundant or overlapping external information: when provided with additional context that reformulates or reiterates knowledge already internalized, they can misallocate attention, resulting in subtle yet systematic declines in performance even when the supplemental material is accurate and expert-curated.

3.5 Ablation Study: Content Quality vs. Information Quantity

To rigorously test whether performance gains stem from information quantity or expert curation quality, we conducted a comprehensive token-matched comparison between AI-generated and expert-reviewed supporting materials. *Tokens* are the fundamental units of text that language models process—roughly corresponding to words or sub-word pieces (e.g., “crystallography” might be split into “crystal” + “lography”). By controlling token count, we ensure that both material types contain equivalent amounts of text, allowing us to isolate content quality effects from simple volume differences. This ablation directly addresses the question: do expert improvements reflect better content or simply more text?

3.5.1 Token-Matched Experimental Design

To isolate the effects of content quality from those of information quantity, we implemented a token-matched ablation study in which every AI-generated supporting passage was paired with its

expert-reviewed counterpart of nearly identical length. This design ensured that both sets of materials provided the same textual volume, allowing any observed performance differences to be directly attributed to qualitative factors such as accuracy, relevance, and pedagogical clarity.

As summarized in Table 5, the mean token count was 566.0 ± 79.2 for AI-generated materials and 568.9 ± 82.7 for expert-reviewed materials, representing a negligible difference of only 2.9 tokens (0.51% change). Moreover, the high correlation ($r = 0.948$) between AI- and expert-reviewed helper lengths across all 217 questions, along with their nearly identical median and interquartile ranges (558.0 [508.0–605.0] vs. 558.0 [513.0–610.0]), confirms that the two distributions are tightly matched.

This strict token control eliminates text volume as a potential confounding factor and establishes a high-fidelity basis for quality-driven comparison. In other words, any measurable performance improvements can be confidently attributed to the qualitative enhancements introduced through expert curation, rather than to variations in the amount of information provided. This methodological precision is critical for disentangling the true impact of expert refinement from superficial gains that might otherwise arise from longer or more verbose passages.

Table 5 Token Count Statistics for Questions and Helper Texts. Expert-reviewed materials maintain virtually identical length to AI-generated materials (mean difference: 2.9 tokens, 0.51%), enabling quality-controlled comparison.

Metric	Questions	AI-Generated	Expert-Reviewed
Mean \pm SD	50.1 ± 15.2	566.0 ± 79.2	568.9 ± 82.7
Median [IQR]	49.0 [38.0–60.0]	558.0 [508.0–605.0]	558.0 [513.0–610.0]
Range	[21–98]	[378–919]	[378–919]
Total	10,882	122,825	123,457
Difference	—	—	+2.9 tokens (+0.51%)
Correlation	—	—	$r = 0.948$

3.5.2 LLM-Based Helper Quality Scoring

To quantitatively validate the qualitative advantages of expert-reviewed helpers, we scored all 217 AI-generated vs. human-reviewed helper pairs using an external rater (GPT-4o-mini via OpenRouter). The rater assigned 0–10 scores on four dimensions aligned with our quality rubric: accuracy, clarity, completeness, and reliability. Human-reviewed passages outperform AI-generated passages by +1.38 to +1.87 points per metric and by +1.72 points on the overall average (Table 6), confirming that expert edits measurably increase helper quality beyond text length controls.

3.5.3 Differential Performance Under Token-Matched Conditions

Table 7 presents a direct comparison of performance gains (Δ) between token-matched AI-generated and expert-reviewed supporting materials across all 74 evaluated models. Despite identical token counts, substantial performance differences emerge, revealing the effect of content quality independent of text volume.

Most models show higher accuracy with expert-reviewed materials, confirming that qualitative improvements—such as en-

hanced conceptual clarity, precise terminology, and improved contextual alignment—produce measurable performance gains even under identical token counts. The strongest relative improvements occur in small models (<7B parameters), which benefit most from the additional clarity and precision introduced by expert curation. For instance, LLaVA-v1.6-mistral-7B improves from +5.54% to +11.07% (+5.53% differential), and mistralai/mistral-7b-instruct-v0.1 exhibits the largest quality-driven transformation (+8.41%), shifting from performance degradation (−5.47%) with AI-generated text to a measurable gain (+2.94%) with expert-reviewed material, under identical token budgets.

Mid-sized models (10–70B) also show clear but smaller improvements, exemplified by LLaVA-v1.6-34B (+5.99% to +11.52%, +5.53% differential). These models possess enough reasoning capacity to leverage higher-quality information but already contain partial crystallographic knowledge, so their absolute gains are moderate.

Conversely, large models (>70B), such as GPT-4.5-preview, O3-mini, and O1, exhibit minimal or slightly negative differences, reflecting a saturation of internal knowledge representations. When most relevant crystallographic concepts are already encoded within the model parameters, additional context contributes little new information and can occasionally disrupt attention alignment or introduce representational interference.

Overall, these results confirm that content quality, not text length, governs open-book performance. Expert review yields the greatest relative benefits for small and mid-sized models, while large models approach a ceiling where additional context produces diminishing or even adverse effects.

Figure 10 summarizes the overall impact of supporting material quality across model size categories. Small models (<7B parameters) achieve the largest relative improvement from expert-reviewed materials, increasing their accuracy by +8.52 percentage points compared to +6.18% with AI-generated content. Mid-sized models (7B–70B) also benefit noticeably, showing a +4.44% gain versus +2.71% with AI-generated materials. In contrast, large models (>70B) display minimal or slightly negative changes with either material type, indicating that their extensive internal knowledge already limits the marginal benefit of added context.

This trend can be explained by differences in knowledge representation and context utilization capacity across model scales. Smaller models lack sufficient internal crystallographic knowledge, so expert-reviewed passages provide missing conceptual structure and precise terminology that directly enhance reasoning accuracy. Mid-sized models already encode partial domain knowledge but still rely on external information to fill gaps, making them responsive to high-quality supporting text. In contrast, very large models possess extensive parametric knowledge, and adding redundant or overlapping context can introduce interference effects, where new information competes with their established internal representations. As a result, they gain little additional benefit and may even experience slight degradation when the external input does not perfectly align with their internal reasoning pathways.

Overall, these findings indicate that while expert curation improves performance across all model scales, the relative gains are most pronounced for small and mid-sized models that can still meaningfully integrate external guidance, whereas large models operate near their knowledge saturation limit.

3.5.3.1 Practical significance of Fig. 10. Improving average accuracy from 72.5% to 79.5% (Fig. 10) is a 7.0 percentage-point gain that lowers the error rate from 27.5% to 20.5%—about a 25% reduction in wrong answers, or roughly 15 additional correct answers on our 217-question benchmark. Moving from 3 wrong answers in 10 to 2 can be noticeable to users because it reduces re-checking and re-asking. However, 79.5% still means 1 in 5 answers is incorrect, so high-stakes crystallography (e.g., indexing, space-group interpretation, experimental planning) should remain human-verified. The main benefit is cost-effective assistance: mid-sized models plus expert-reviewed hints approach large-model accuracy at lower compute cost.

3.5.4 Quantity-Driven Effects: Evidence from Token Budget Constraints

To further disentangle quality from quantity effects, Section 3.7 presents complementary evidence that information quantity alone can degrade performance. Our token budget analysis (Figure 11) reveals that llama-3-chat’s open-book accuracy dropped from 36.87% at 256 tokens to 26.73% at 2048+ tokens—a 10 percentage point degradation—when provided with longer supporting materials. This inverse relationship demonstrates severe token starvation: the model exhausts its computational budget on input processing, leaving insufficient capacity for answer generation. The supporting materials, rather than aiding reasoning, become a computational burden that crowds out response formulation.

This finding establishes a critical control, if performance gains stemmed primarily from text volume rather than content quality, we would not observe degradation with increased token budgets in resource-constrained models. The token starvation phenomenon proves that “more text” does not guarantee better outcomes and, in fact, can be counterproductive when models lack the capacity to efficiently process additional context.

3.5.5 Interpretation: Quality, Not Quantity, Drives Improvements

The combination of token-matched comparisons (identical length, differential outcomes) and token budget analysis (increased length, degraded outcomes) provides convergent evidence that content quality—specifically, accuracy, relevance, and pedagogical clarity—drives the observed performance improvements, not mere text volume. Expert-reviewed materials successfully addressed the limitations identified in AI-generated content: technical inaccuracies, insufficient depth, tangential information, and suboptimal pedagogical framing. These qualitative enhancements enable mid-capacity models to better integrate external knowledge, bridging the gap between their processing capability and incomplete domain expertise.

Critically, the token-matched design ensures that expert improvements cannot be attributed to providing “more information”

in terms of token count. Instead, expert review enhances information density, precision, and alignment with question-specific reasoning needs—dimensions of quality orthogonal to text length. This ablation establishes that the OPENXRD framework’s performance gains reflect genuine knowledge enhancement rather than computational artifacts of longer context windows.

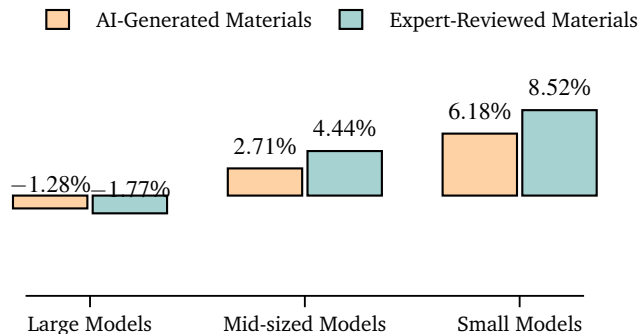


Fig. 10 Average performance gains from AI-generated vs. expert-reviewed supporting materials across model size categories. Large Models (>70B parameters or advanced architectures like GPT-4, GPT-5, O1, O3-mini, n=27); Mid-sized Models (>7B-70B parameters including LLaVA-34B, QWEN2-7B, Mistral variants, n=27); Small Models (\leq 7B parameters including QWEN2-0.5B, LLaMA-3.2-3B, LLaVA-7B, LLaMAT variants, Honeybee-7B, n=20). Note that large models show performance degradation with supporting materials, while mid-sized and small models benefit substantially from expert-reviewed materials. Overall, these results show that as models become larger and contain more built-in knowledge, the additional benefit from external information gradually diminishes.

3.6 Detailed Subtask-Level Performance with Expert-Reviewed Materials

To gain deeper insights, we examined *subtask-level* performance with expert-reviewed materials. Table 8 shows how LLaVA-onevision-QWEN2-7B-ov behaves on key XRD subtasks. The rationale for selecting this model is its substantial enhancement from expert-reviewed materials, which offers valuable insights into the limits of performance improvement. For several subtasks such as Crystal Structure, Laue Patterns, Metal Structures, and Powder Diffraction, expert-reviewed materials transformed performance from complete failure (0%) to perfect accuracy (100%). Expert materials particularly improved performance on structural tasks, enhancing Structure Factors by 25% and Coordination Numbers by 40%. However, complex mathematical derivations like Bragg’s Law and Calculation Methods remained challenging even with expert materials, suggesting that some concepts require more than textual explanation. An illustrative example is the question "What is the structure factor F for a base-centered unit cell when h and k are mixed (one even, one odd)?" Correct answer is being $F = f$, while a model consistently selecting $F = 2f$, reveals that it has not internalized how lattice symmetry produces systematic absences, an error that echoes its 0% score on Bragg’s Law questions. Additionally, for a few subtasks where the model had strong initial performance, such as Complex Mathematics and Wave Scattering, supporting materials appeared to interfere with

the model’s existing knowledge.

Mathematically intensive subtasks including Bragg’s Law derivations, structure factor calculations, and reflection condition analysis showed universal 0% improvement with supporting materials across all 74 models. For instance, when asked about structure factors for base-centered lattices with mixed h,k indices, models consistently failed to execute the symbolic computation $F = f[1 + e^{i\pi(h+k)}]$ despite correct textual explanations, revealing that current LLMs cannot perform the formal algebraic operations required for crystallographic problem-solving.

3.7 Impact of Token Budget Constraints on Open-Book Performance

While the previous analyses examined model performance under standard inference conditions, we now investigate how computational constraints—specifically, output token budget limitations—affect models’ ability to leverage external knowledge. Token budget restrictions are particularly relevant in deployment scenarios where computational resources or API costs impose practical limits on generation length. Understanding how these constraints interact with open-book augmentation is crucial for real-world applications.

We systematically evaluated two models across varying maximum token budgets (256 to 4096 tokens): llama3-chat, a 7B-parameter specialized model, and O3-mini, a reasoning-optimized model designed for scientific tasks. Figure 11 presents the accuracy trends as token budgets increase.

The results reveal markedly different patterns between the two models. For llama3-chat (Figure 11a), closed-book performance remains relatively stable across token budgets (55-58%), showing minimal sensitivity to generation length constraints. However, open-book performance exhibits a counterintuitive decline: accuracy drops from 36.87% at 256 tokens to 26.73% at 2048+ tokens—a degradation of approximately 10 percentage points. This inverse relationship suggests severe token starvation: as the model attempts to process longer supporting materials, it exhausts its token budget on input comprehension and internal reasoning, leaving insufficient capacity for coherent answer generation. The supporting materials, rather than aiding reasoning, become a computational burden that crowds out the model’s ability to formulate responses.

In contrast, O3-mini (Figure 11b) demonstrates more favorable scaling properties. Closed-book accuracy improves substantially from 77.42% at 256 tokens to a peak of 95.39% at 2560 tokens, indicating the model benefits from additional reasoning space for complex crystallographic problems. Open-book performance similarly improves from 80.65% to approximately 90%, stabilizing around 1024 tokens. The gap between closed-book and open-book performance narrows at higher token budgets, suggesting that O3-mini can more effectively integrate external knowledge when given adequate computational headroom. However, even O3-mini shows slight performance degradation beyond 2560 tokens in closed-book mode, hinting at potential overfitting or unnecessary elaboration when unconstrained.

These findings have important implications for deployment

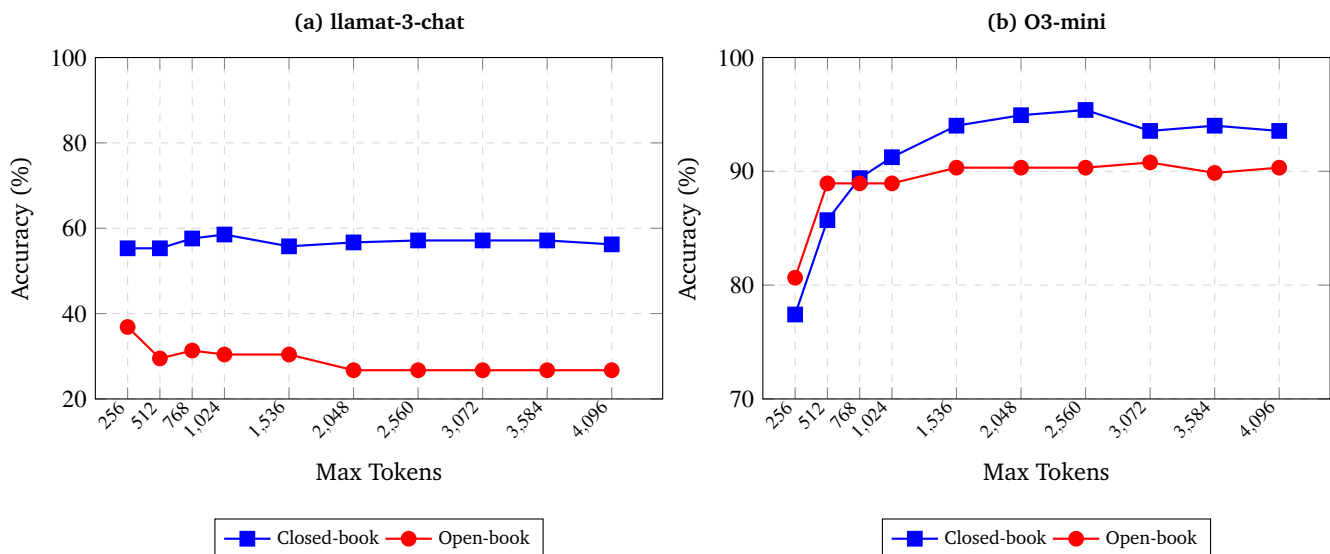


Fig. 11 Impact of token budget constraints on closed-book and open-book performance for (a) llama-3-chat and (b) O3-mini. The x-axis shows maximum output tokens allowed, while the y-axis shows accuracy on the 217-question benchmark. Note the different y-axis scales: llama-3-chat ranges 20-100% while O3-mini ranges 70-100% due to their different baseline capabilities.

strategies. First, token budget selection requires careful calibration: smaller models like llama-3-chat exhibit pathological behavior under open-book conditions when token budgets exceed their processing capacity, while more capable models like O3-mini require minimum token budgets (1024 tokens) to effectively leverage external materials. Second, the phenomenon of "open-book degradation" in resource-constrained models suggests that naively providing supporting materials without ensuring sufficient token allocation for answer synthesis can be counterproductive. Third, the results underscore fundamental architectural differences: reasoning-optimized models (O3-mini) appear better equipped to manage the token allocation trade-off between comprehending external context and generating accurate responses.

From a practical standpoint, these observations suggest that effective open-book augmentation requires not only high-quality supporting materials but also appropriate computational provisioning. For deployment scenarios with strict token limits, practitioners should either: (1) use models specifically designed for reasoning tasks that can efficiently allocate tokens between context processing and response generation, (2) employ adaptive token budgets that scale with input complexity, or (3) pre-process supporting materials to reduce their token footprint while preserving essential information. Future work should investigate token allocation strategies that dynamically balance between context comprehension and response generation, potentially through attention mechanism modifications or explicit token budgeting protocols.

4 Discussion

Our results show that using domain-specific prompts, or open-book mode, significantly enhances question-answering accuracy in crystallography. This is especially true for smaller or more general models, where the additional context helps fill knowledge gaps. However, the quality and relevance of the supporting tex-

tual material are crucial. In some instances, the material generated by GPT-4.5 did not align well with the question's needs, causing confusion or contradictory information. This underscores the importance of relevance filtering or validation of supporting material before it is used.

While OPENXRD focuses on inference-time context assimilation, it is explicitly designed to complement parameter-efficient fine-tuning (PEFT) approaches. PEFT methods can encode crystallographic knowledge directly into model weights through techniques like LoRA⁶⁰, whereas OPENXRD diagnoses whether models—adapted or not—can effectively utilize answer-guiding context that does not directly reveal solutions. A comprehensive evaluation strategy might compare: (i) closed-book performance after PEFT on external XRD corpora, (ii) open-book performance after PEFT using our oracle passages, and (iii) our baseline open-book performance without PEFT. This three-way comparison decomposes gains attributable to parametric adaptation versus gains from inference-time guidance, a separation difficult to obtain in end-to-end training studies. For instance, a PEFT-adapted model that shows minimal open-book improvement might indicate successful knowledge internalization, while a model showing large open-book gains suggests incomplete adaptation where external guidance remains valuable. OPENXRD standardizes this diagnostic capability across architectures and scales.

Advanced mathematical reasoning remains a challenge. Our analysis indicates that open-book mode rarely resolves complex mathematical problems, such as structure factor calculations or multi-step interference proofs. Future enhancements could include integrating symbolic math modules or domain-specific solvers to better handle these tasks, rather than relying solely on textual references.

The complexity of visual data in crystallography, such as tabulated results, diffraction patterns, and annotated structural diagrams, presents additional challenges. Accurate extraction of this

information requires improvements in optical character recognition (OCR), figure parsing, and multi-modal alignment. Developing tailored visual backbones or domain-tuned OCR engines will be essential for applying our methods to real-world scenarios, like analyzing lab notebooks or older textbook scans.

Text-based supporting materials prove insufficient for mathematically intensive subtasks requiring symbolic manipulation. Consider a diagnostic case from our benchmark: “For a base-centered unit cell, what is the structure factor F when h and k are mixed (one even, one odd)?” Despite expert-reviewed materials correctly explaining that atoms at $(0,0,0)$ and $(1/2,1/2,0)$ produce destructive interference when h and k have mixed parity (yielding $F=0$), multiple frontier models incorrectly answered $F=2f$. Analysis reveals they cannot maintain intermediate symbolic states during phase calculations $\phi = 2\pi(hx + ky + lz)$ or correctly apply $F = f[1 + e^{i\pi(h+k)}] = 0$ when $(h+k)$ is odd. This failure extends to Bragg’s Law derivations, structure factor algebra, and powder diffraction indexing—all showing 0% improvement across our 74-model evaluation regardless of size or architecture.

To overcome this architectural limitation, future work should integrate LLMs with symbolic computation engines such as SymPy¹⁰⁶ or Wolfram Alpha¹⁰⁷ for exact algebraic manipulations, crystallographic knowledge graphs encoding systematic absence rules and space group constraints as structured logical representations rather than text, and domain-specific software including GSAS-II¹⁰⁸ for powder diffraction refinement and Mercury¹⁰⁹ for structure visualization. Such hybrid architectures would enable the LLM to parse problems linguistically, delegate mathematical operations to specialized modules, and synthesize results—combining linguistic flexibility with computational rigor. This approach extends beyond crystallography to other physics-heavy domains requiring both conceptual reasoning and mathematical precision.

In parallel, a notable tension exists between generalist and specialist models. While larger LLMs like GPT-4 and GPT-4.5 have broad knowledge, they often miss the nuances of specific domains that specialized models capture more effectively. A hybrid approach, where a specialist model generates domain-specific references for a generalist model, could offer a powerful solution. Additionally, ethical and copyright considerations must be managed carefully, especially as we look to expand these systems to other technical fields with extensive proprietary literature.

Our research identifies two primary methods for enhancing model performance with domain expertise: directly embedding knowledge into large models, such as frontier models like GPT-5, GPT-4.5, and O3-mini, and providing models with access to expert-reviewed references during inference. This latter strategy proves especially useful for mid-capacity models, enabling them to nearly match the performance of their larger counterparts by leveraging a “knowledge bridge.”

For example, a medium-sized model like LLaVA-v1.6-34B, when paired with expert materials, achieves 78.34% accuracy, approaching the performance of much larger models like Llama-3.1-405B (84.33%) and even surpassing some frontier models in cost-effectiveness but with far fewer resources required. The integration of expert-reviewed domain knowledge is not only ben-

eficial in textual analysis but also in multi-modal contexts such as medical imaging or geospatial analysis, where expert-reviewed context can similarly boost specialized question-answering performance and unlock new application areas.

However, the addition of external information is not always beneficial. For instance, multiple frontier models show performance degradation with expert-reviewed supporting materials: GPT-4.5-preview (-3.23%), GPT-5 (-3.68%), Grok-4-fast (-5.78%), Claude-3.5-Sonnet (-1.84%), and dziner-qwen-2.5-72b (-4.14%), possibly due to conflicts with their pre-trained internal knowledge. This suggests that more information is not necessarily better, particularly for top-tier models that have been extensively trained, as the interference from external context can disrupt their already-comprehensive internal reasoning processes.

Our results show that both small and mid-sized models benefit from external knowledge, with small models exhibiting the largest relative gains, whereas large models experience interference. This reveals a fundamental insight: external knowledge augmentation is most effective within a specific capability range where models have sufficient processing power but incomplete domain coverage. This finding has important implications for cost-effective deployment strategies in specialized scientific domains.

Future research should focus on automated methods to determine when expert review is most beneficial, multi-stage approaches for targeted expert review, and the potential for fine-tuning models to better utilize external references, as well as mechanisms to detect when models have sufficient internal knowledge that external context becomes counterproductive.

Beyond incremental improvements, addressing the universal mathematical reasoning failures documented in our benchmark requires architectural innovation. Hybrid systems coupling LLMs with symbolic algebra engines, structured crystallographic knowledge graphs encoding lattice symmetries and systematic absence rules, and specialized software for diffraction simulation and structure refinement would enable models to delegate exact computations while maintaining linguistic problem-solving capabilities. Multi-modal extensions incorporating actual XRD patterns and crystal structure visualizations would test whether vision-language models can integrate visual and textual information. Dynamic retrieval replacing oracle passages with corpus-retrieved content would decompose RAG accuracy into retrieval versus assimilation components. Fine-tuning studies using OPENXRD before and after domain adaptation would reveal whether parametric knowledge embedding complements or supersedes inference-time guidance. Cross-domain validation in related scattering techniques and computational chemistry would test whether our findings about model capacity and external knowledge effectiveness generalize beyond crystallography.

In parallel, we are developing an open-ended XRD evaluation set (short-answer and problem-solving tasks) to complement OPENXRD’s multiple-choice diagnostic benchmark and to enable qualitative assessment of explanation quality and reasoning depth.

Despite these advancements, certain limitations remain. Complex mathematical concepts and advanced tasks like reflection or

symmetry analysis still pose challenges, as models do not always fully grasp these concepts through text-based materials alone. Moreover, there are instances where supporting materials can detract from a model’s performance if they do not align perfectly with the model’s pre-existing knowledge base.

Given these limitations, the reliance of open-book question answering on human-curated content may be difficult to sustain across all fields, and the uneven gains observed across model sizes underscore the need for further work on how best to select, refine, and integrate external knowledge.

5 Conclusions

The OPENXRDbenchmark provides a controlled and extensible framework for evaluating how large language models (LLMs) and multimodal LLMs integrate external scientific knowledge. Through token-matched experiments and token-budget analyses, the study isolates the effect of content quality from text quantity and reveals that expert-reviewed supporting materials consistently enhance model accuracy, even when passage length is identical. Small and mid-sized models both exhibit clear accuracy improvements when augmented with expert-reviewed materials, with the relative gain being most pronounced for small models, whereas large models show minimal or slightly negative changes due to knowledge saturation. These findings demonstrate that as model capacity increases, the relative advantage of external context diminishes, even though overall accuracy continues to scale with size.

Beyond these controlled experiments, OPENXRDR demonstrates strong scalability and generalizability across 74 diverse model architectures, including general-purpose systems (GPT, Claude), reasoning-optimized models (O-series), code-specialized variants (QWEN-coder), domain-adapted frameworks (LLaMAT, dZiner), and vision-language models (LLaVA). This diversity confirms that OPENXRDR is model-agnostic, functioning as a diagnostic layer for both closed-book and retrieval-augmented reasoning systems. For instance, the code-specialized model QWEN3-coder-plus improved dramatically, from 22.99% in the closed-book setting (Table 2) to 88.94% in the open-book setting (Table 4) with expert-reviewed materials, demonstrating that OPENXRDR’s insights extend beyond language-only systems and generalize effectively across diverse architectural paradigms. Moreover, because OPENXRDR isolates inference-time reasoning while remaining compatible with dynamic retrieval pipelines, it can be directly extended into a deployable RAG-evaluation suite that separates retrieval quality from assimilation capability.

We therefore do not report a single “standard RAG baseline” in this work, because end-to-end RAG accuracy depends strongly on retriever choice, corpus construction, chunking, and ranking, which would introduce additional confounds beyond the generator-side assimilation question studied here. Instead, OPENXRDR provides the oracle-context upper bound and a controlled harness that can later be paired with retrieved chunks to decompose end-to-end RAG performance into retrieval quality versus generator assimilation.

Finally, the framework’s practical deployment insights show how these findings can guide real-world applications. OPENXRDR

identifies mid-sized models (7B–70B parameters) augmented with expert-reviewed passages as an optimal balance between cost and performance, approaching or even matching large-model accuracy while requiring significantly fewer computational resources. This provides a cost-effective deployment pathway for organizations with limited budgets. The framework also enables the design of adaptive token-budget strategies that scale with task complexity, along with pre-processing approaches that reduce token usage while preserving essential information. Such model-selection and resource-allocation guidelines directly address the economic and computational realities of deploying AI systems at scale.

In conclusion, OPENXRDR is not an artificial or static experiment, but a reproducible, extensible, and practically informative framework. It quantifies how model capacity, resource budgets, and content quality interact under real-world constraints, provides scalable and legally compliant data generation methods, and delivers empirical evidence to support efficient design of open-book and retrieval-augmented reasoning systems. The framework’s diagnostic capabilities empower organizations to make informed decisions about when to scale model size versus when to enhance smaller models with curated external knowledge, thereby advancing both the scientific understanding and the practical deployment of domain-specialized language models.

Author contributions

A.V. and A.S. contributed equally to this work as co-first authors. A.V.: Conceptualization, Methodology, Software, Formal analysis, Investigation, Data curation, Writing – original draft, Visualization. A.S.: Conceptualization, Methodology, Data curation, Investigation, Validation, Writing – review & editing. A.S. designed the crystallography question set and led the expert review process for GPT-generated questions. Z.Z., Y.X., and G.H.: Methodology, Software, Investigation, Validation, Writing – review & editing. Z.Z., Y.X., and G.H. provided substantial contributions to model development, experimental design improvements, and participated in the expert review and refinement of GPT-generated questions to ensure scientific accuracy. C.X. and N.A.: Conceptualization, Supervision, Project administration, Resources, Writing – review & editing, Funding acquisition. C.X. and N.A. jointly led and supervised the project, providing strategic direction and ensuring research quality throughout all phases of the work.

Conflicts of interest

The authors declare that they have no competing financial interests or personal relationships that could have appeared to influence the work reported in this document.

Data availability

The complete dataset of 217 expert-curated crystallography questions, supporting materials (both AI-generated and expert-reviewed versions), evaluation scripts, and model implementation code are publicly available at <https://github.com/niaz60/OpenXRDR>. Additional project information and resources can be found at <https://niaz60.github.io/OpenXRDR/>. The repository includes detailed documentation for reproducing all experimental

Table 2 Comprehensive "closed-book mode" accuracy results on the 217-item crystallography QA benchmark, including older GPT-4 variants and newly reported models. The rightmost column shows model parameter sizes: B = billions, T = trillions, U = undisclosed. For Mixture-of-Experts (MoE) models, format is total/active parameters. Estimated values marked with ~, N/A for routing services.

Rank	Model (Closed-book mode)	Acc. (%)	Correct	Params
1	openai/gpt-5	96.77	210/217	~300B
2	x-ai/grok-4-fast	96.31	209/217	U
2	openai/gpt-5-codex	96.31	209/217	~300B
4	google/gemini-2.5-pro	95.39	207/217	U
5	o3-mini	93.55	203/217	U
6	meituan/longcat-flash-chat	93.09	202/217	560B/27B
7	gpt-4.5-preview	92.63	201/217	U
8	anthropic/claude-3.5-sonnet	91.24	198/217	~175B
9	openai/gpt-4o	90.74	196/216	~200B
10	dziner-qwen-2.5-72b	90.32	196/217	~72B
10	perplexity/sonar-pro	90.32	196/217	70B
10	qwen/qwen3-next-80b-a3b-instruct	90.32	196/217	80B/3B
13	deepseek/deepseek-v3.1-terminus	89.86	195/217	671B/37B
13	qwen/qwen-plus	89.86	195/217	U
13	qwen/qwen3-next-80b-a3b-thinking	89.86	195/217	80B/3B
16	deepseek/deepseek-chat	89.40	194/217	671B/37B
16	o1	89.40	194/217	~200B
16	qwen/qwen-max	89.40	194/217	U
19	anthropic/claude-3-opus	88.94	193/217	U
20	openai/o1-mini	88.02	191/217	~100B
21	meta-llama/llama-3.1-405b-instruct	87.56	190/217	405B
21	qwen/qwen-2.5-72b-instruct	87.56	190/217	72B
23	mistralai/mistral-large	86.18	187/217	123B
24	amazon/nova-pro-v1	86.11	186/216	~90B
25	gpt-4-turbo	85.25	185/217	1.8T/280B
26	meta-llama/llama-3-70b-instruct	84.79	184/217	70B
26	meta-llama/llama-3.1-70b-instruct	84.79	184/217	70B
28	dziner-qwen-2.5-coder-32b	83.87	182/217	~32B
29	openai/gpt-4-0314	83.41	181/217	1.8T/280B
29	gpt-4-turbo-preview	83.41	181/217	1.8T/280B
31	amazon/nova-lite-v1	82.03	178/217	~20B
32	dziner-qwen-2.5-7b	81.57	177/217	~7B
32	gpt-4	81.57	177/217	1.8T/280B
34	openai/gpt-4o-mini	81.11	176/217	~8B
34	openrouter/auto	81.11	176/217	N/A
36	qwen/qwen-2.5-7b-instruct	79.72	173/217	7B
37	google/gemma-2-27b-it	79.26	172/217	27B
38	anthropic/claude-3.5-haiku	77.57	166/214	U
39	mistralai/mixtral-8x22b-instruct	76.81	159/207	141B/39B
40	mistralai/mistral-7b-instruct	75.35	162/215	7B
41	google/gemma-2-9b-it	75.12	163/217	9B
42	amazon/nova-micro-v1	74.65	162/217	~11B
42	mistralai/mistral-small	74.65	162/217	24B
44	anthropic/claude-3-haiku	74.04	154/208	~20B
45	openai/gpt-3.5-turbo-16k	72.60	151/208	~20B
46	mistralai/mixtral-8x7b-instruct	72.33	149/206	47B/13B
47	meta-llama/llama-3-8b-instruct	71.89	156/217	8B
48	mistralai/pixtral-12b	71.83	153/213	12B
49	openai/gpt-3.5-turbo	70.67	147/208	~20B
50	meta-llama/llama-3.1-8b-instruct	69.12	150/217	8B
51	llava-v1.6-34b	66.82	145/217	34B
52	lmms-lab/llava-onevision-qwen2-7b-si	66.36	144/217	7B
53	lmms-lab/llava-onevision-qwen2-7b-ov-chat	65.90	143/217	7B
54	lmms-lab/llava-onevision-qwen2-7b-ov	65.44	142/217	7B
55	meta-llama/llama-3.2-3b-instruct	64.98	141/217	3B
56	arcee-ai/afm-4.5b	62.21	135/217	4.5B
57	mistralai/mistral-7b-instruct-v0.1	59.50	119/200	7B
58	perplexity/sonar	59.24	125/211	70B
59	undi95/remm-slerp-l2-13b	57.08	121/212	13B
60	llamat-3-chat	57.14	124/217	8B
61	alibaba/tongyi-deepresearch-30b-a3b	55.76	121/217	30B/3B
62	gryphe/mythomax-l2-13b	53.77	114/212	13B
63	llava-v1.6-mistral-7b	52.99	115/217	7B
64	llamat-2-chat	50.69	110/217	7B
65	lmms-lab/llava-onevision-qwen2-0.5b-ov	47.47	103/217	0.5B
66	llava-v1.5-13b	46.54	101/217	13B
67	lmms-lab/llava-onevision-qwen2-0.5b-si	46.08	100/217	0.5B
68	qwen/qwen3-coder-flash	43.46	83/191	U
69	qwen/qwen3-coder-plus	22.99	43/187	U
70	honeybee-13b	22.12	48/217	13B
71	qwen/qwen-2.5-coder-32b-instruct	21.03	45/214	32B
72	honeybee-7b	19.35	42/217	7B
73	llava-v1.5-7b	17.97	39/217	7B
74	llamat-2	16.59	36/217	7B

results presented in this study.

Acknowledgments

We gratefully acknowledge financial support from multiple sources. A.V., G.H., C.X., and N.A. received support from the National Nuclear Security Administration (NNSA) under grant NA0004078. A.S., Z.Z., Y.X., C.X., and N.A. were supported by the National Science Foundation (NSF) under grant 2202124. Additional funding for N.A. was provided by the Department of Energy (DOE) under award DE-SC0020340. We thank the crystallography experts who participated in the review and validation of our question dataset. We also acknowledge the computational resources and infrastructure that enabled the extensive model evaluations presented in this work.

References

- Bob B He. *Two-dimensional X-ray Diffraction*. John Wiley & Sons, 2018.
- Ishan Rathore, Vandana Mishra, and Prasenjit Bhaumik. Advancements in macromolecular crystallography: From past to present. *Emerging Topics in Life Sciences*, 5(1):127–149, 2021.
- Rick Uvic. *Crystallography and Crystal Chemistry*. Springer, 2024.
- Boris K Vainshtein. *Fundamentals of crystals: symmetry, and methods of structural crystallography*, volume 1. Springer Science & Business Media, 2013.
- Ulrich Müller and Gemma De La Flor. *Symmetry relationships between crystal structures: applications of crystallographic group theory in crystal chemistry*, volume 24. Oxford University Press, 2024.
- Dierk Raabe. The materials science behind sustainable metals and alloys. *Chemical reviews*, 123(5):2436–2608, 2023.
- Gözde Altuntaş, Onur Altuntaş, M Kemal Öztürk, and Bülent Bostan. Metallurgical and crystallographic analysis of different amounts of deformation applied to hadfield steel. *International Journal of Metalcasting*, 17(2):1340–1349, 2023.
- Vanessa Bijak, Michal Szczygiel, Joanna Lenkiewicz, Michal Gucwa, David R Cooper, Krzysztof Murzyn, and Wlodek Minor. The current role and evolution of x-ray crystallography in drug discovery and development. *Expert opinion on drug discovery*, 18(11):1221–1230, 2023.
- Shakil N Afraj, Chia-Chi Lin, Arulmozhi Velusamy, Chang-Hui Cho, Hsin-Yi Liu, Jianhua Chen, Gene-Hsiang Lee, Jui-Chen Fu, Jen-Shyang Ni, Shih-Huang Tung, et al. Heteroalkyl-substitution in molecular organic semiconductors: chalcogen effect on crystallography, conformational lock, and charge transport. *Advanced Functional Materials*, 32(27):2200880, 2022.
- Satoru Inoue, Kiyoshi Nikaido, Toshiki Higashino, Shunto Arai, Mutsuo Tanaka, Reiji Kumai, Seiji Tsuzuki, Sachio Horiuchi, Haruki Sugiyama, Yasutomo Segawa, et al. Emerging disordered layered-herringbone phase in organic semicon-

Table 3 Comparison of model accuracy in closed-book mode vs. open-book mode with AI-generated supporting materials. $\Delta = (\text{Open-book mode}) - (\text{Closed-book mode})$.

Model	Closed-book mode (%)	Open-book mode (%)	Δ
openai/gpt-5	96.77	94.93	-1.84
x-ai/grok-4-fast	96.31	95.39	-0.92
openai/gpt-5-codex	96.31	94.47	-1.84
google/gemini-2.5-pro	95.39	88.48	-6.91
o3-mini	93.55	89.40	-4.15
meituan/longcat-flash-chat	93.09	90.32	-2.77
gpt-4.5-preview	92.63	90.32	-2.31
anthropic/claude-3.5-sonnet	91.24	89.40	-1.84
openai/gpt-4o	90.74	87.56	-3.18
dziner-qwen-2.5-72b	90.32	87.10	-3.22
perplexity/sonar-pro	90.32	90.32	+0.00
qwen/qwen3-next-80b-a3b-instruct	90.32	89.40	-0.92
deepseek/deepseek-v3.1-terminus	89.86	90.78	+0.92
qwen/qwen-plus	89.86	90.78	+0.92
qwen/qwen3-next-80b-a3b-thinking	89.86	87.10	-2.76
deepseek/deepseek-chat	89.40	91.24	+1.84
o1	89.40	88.02	-1.38
qwen/qwen-max	89.40	88.02	-1.38
anthropic/claude-3-opus	88.94	88.02	-0.92
openai/o1-mini	88.02	88.48	+0.46
meta-llama/llama-3.1-405b-instruct	87.56	82.95	-4.61
qwen/qwen-2.5-72b-instruct	87.56	86.18	-1.38
mistralai/mistral-large	86.18	83.87	-2.31
amazon/nova-pro-v1	86.11	86.64	+0.53
gpt-4-turbo	85.25	85.71	+0.46
meta-llama/llama-3-70b-instruct	84.79	80.65	-4.14
meta-llama/llama-3.1-70b-instruct	84.79	83.41	-1.38
dziner-qwen-2.5-coder-32b	83.87	84.79	+0.92
openai/gpt-4-o314	83.41	77.42	-5.99
gpt-4-turbo-preview	83.41	82.49	-0.92
amazon/nova-lite-v1	82.03	84.79	+2.76
dziner-qwen-2.5-7b	81.57	79.26	-2.31
gpt-4	81.57	82.03	+0.46
openai/gpt-4o-mini	81.11	82.03	+0.92
openrouter/auto	81.11	81.57	+0.46
qwen/qwen-2.5-7b-instruct	79.72	75.12	-4.60
google/gemma-2-27b-it	79.26	78.80	-0.46
anthropic/claude-3.5-haiku	77.57	88.02	+10.45
mistralai/mixtral-8x22b-instruct	76.81	80.09	+3.28
mistralai/mistral-7b-instruct	75.35	77.42	+2.07
google/gemma-2-9b-it	75.12	77.42	+2.30
amazon/nova-micro-v1	74.65	79.26	+4.61
mistralai/mistral-small	74.65	79.26	+4.61
anthropic/claude-3-haiku	74.04	82.49	+8.45
openai/gpt-3.5-turbo-16k	72.60	71.01	-1.59
mistralai/mixtral-8x7b-instruct	72.33	75.96	+3.63
meta-llama/llama-3-8b-instruct	71.89	73.27	+1.38
mistralai/pixtral-12b	71.83	75.58	+3.75
openai/gpt-3.5-turbo	70.67	71.50	+0.83
meta-llama/llama-3.1-8b-instruct	69.12	75.12	+6.00
llava-v1.6-34b	66.82	72.81	+5.99
lms-lab/llava-onevision-qwen2-7b-si	66.36	71.89	+5.53
lms-lab/llava-onevision-qwen2-7b-ov-chat	65.90	72.35	+6.45
lms-lab/llava-onevision-qwen2-7b-ov-ov	65.44	71.43	+5.99
meta-llama/llama-3.2-3b-instruct	64.98	62.67	-2.31
arcee-ai/afm-4.5b	62.21	64.52	+2.31
mistralai/mistral-7b-instruct-v0.1	59.50	54.03	-5.47
perplexity/sonar	59.24	68.84	+9.60
undi95/remm-slerp-l2-13b	57.08	61.50	+4.42
llamat-3-chat	57.14	30.41	-26.73
alibaba/tongyi-deepresearch-30b-a3b	55.76	80.18	+24.42
gryphe/mythomax-l2-13b	53.77	61.68	+7.91
llava-v1.6-mistral-7b	52.99	58.53	+5.54
llamat-2-chat	50.69	21.13	-29.56
lms-lab/llava-onevision-qwen2-0.5b-ov	47.47	51.15	+3.68
llava-v1.5-13b	46.54	44.24	-2.30
lms-lab/llava-onevision-qwen2-0.5b-si	46.08	51.15	+5.07
qwen/qwen3-coder-flash	43.46	84.33	+40.87
qwen/qwen3-coder-plus	22.99	88.94	+65.95
honeybee-13b	22.12	23.04	+0.92
qwen/qwen-2.5-coder-32b-instruct	21.03	27.01	+5.98
honeybee-7b	19.35	23.04	+3.69
llava-v1.5-7b	17.97	23.96	+5.99
llamat-2	16.59	19.82	+3.23

ductors unveiled by electron crystallography. *Chemistry of Materials*, 34(1):72–83, 2021.

- 11 Bernard Dennis Cullity and RJPT Smoluchowski. Elements of x-ray diffraction. *Physics Today*, 10(3):50–50, 1957.
- 12 Asif Ali, Yi Wai Chiang, and Rafael M Santos. X-ray diffraction techniques for mineral characterization: A review for engineers of the fundamentals, applications, and research directions. *Minerals*, 12(2):205, 2022.
- 13 Andrei A Bunaciu, Elena Gabriela UdrişTioiu, and Hassan Y Aboul-Enein. X-ray diffraction: instrumentation and applications. *Critical reviews in analytical chemistry*, 45(4):289–

299, 2015.

- 14 Brian Cantor. *The equations of materials*. Oxford University Press, 2020.
- 15 Lawrence Bragg. X-ray crystallography. *Scientific American*, 219(1):58–74, 1968.
- 16 Christopher G Pope. X-ray diffraction and the bragg equation. *Journal of chemical education*, 74(1):129, 1997.
- 17 Joachim Stöhr. *The nature of X-rays and their interactions with matter*. Number PUBDB-2024-05989. Springer, 2023.
- 18 Siti Fatimah, Risti Ragadhita, Dwi Fitria Al Husaeni, and Asep Bayu Dani Nandiyanto. How to calculate crystallite size from x-ray diffraction (xrd) using scherrer method. *ASEAN Journal of Science and Engineering*, 2(1):65–76, 2022.
- 19 Jin-Woong Lee, Woon Bae Park, Minseuk Kim, Satendra Pal Singh, Myoung-ho Pyo, and Kee-Sun Sohn. A data-driven xrd analysis protocol for phase identification and phase-fraction prediction of multiphase inorganic compounds. *Inorganic Chemistry Frontiers*, 8(10):2492–2504, 2021.
- 20 Vladimir Uvarov. The influence of x-ray diffraction pattern angular range on rietveld refinement results used for quantitative analysis, crystallite size calculation and unit-cell parameter refinement. *Applied Crystallography*, 52(2):252–261, 2019.
- 21 Kai He, Nuofu Chen, Congjie Wang, Lishuai Wei, and Jikun Chen. Method for determining crystal grain size by x-ray diffraction. *Crystal Research and Technology*, 53(2):1700157, 2018.
- 22 Shelan Salm Sadiq Qadr. Calculating thin film strain from xrd data. *Academia Open*, 8(2):10–21070, 2023.
- 23 Simone Dolabella, Aurelio Borzi, Alex Dommann, and Antonia Neels. Lattice strain and defects analysis in nanostructured semiconductor materials and devices by high-resolution x-ray diffraction: theoretical and practical aspects. *Small Methods*, 6(2):2100932, 2022.
- 24 Jerardo E Salgado, Samuel Lerman, Zhaotong Du, Chenliang Xu, and Niaz Abdolrahim. Automated classification of big x-ray diffraction data using deep learning models. *npj Computational Materials*, 9(1):214, 2023.
- 25 Angelo Ziletti, Devinder Kumar, Matthias Scheffler, and Luca M Ghiringhelli. Insightful classification of crystal structures using deep learning. *Nature communications*, 9(1):2775, 2018.
- 26 Woon Bae Park, Jiyong Chung, Jaeyoung Jung, Keemin Sohn, Satendra Pal Singh, Myoung-ho Pyo, Namsoo Shin, and K-S Sohn. Classification of crystal structure using a convolutional neural network. *IUCrJ*, 4(4):486–494, 2017.
- 27 Juan Iván Gómez-Peralta, Kim Bokhimi, and Patricia Quintana. Convolutional neural networks to assist the assessment of lattice parameters from x-ray powder diffraction. *The Journal of Physical Chemistry A*, 127(36):7655–7664, 2023.
- 28 Abhik Chakraborty and Raksha Sharma. A deep crystal structure identification system for x-ray diffraction patterns. *The Visual Computer*, 38(4):1275–1282, 2022.
- 29 Jin-Woong Lee, Woon Bae Park, Jin Hee Lee, Satendra Pal Singh, and Kee-Sun Sohn. A deep-learning technique for

Table 4 Comparison of model accuracy in closed-book mode vs. open-book mode with expert-reviewed supporting materials. $\Delta = (\text{Open-book mode}) - (\text{Closed-book mode})$.

Model	Closed-book mode (%)	Open-book mode (%)	Δ
openai/gpt-5	96.77	93.09	-3.68
x-ai/grok-4-fast	96.31	90.53	-5.78
openai/gpt-5-codex	96.31	92.17	-4.14
google/gemini-2.5-pro	95.39	92.63	-2.76
o3-mini	93.55	89.86	-3.69
meituan/longcat-flash-chat	93.09	89.86	-3.23
gpt-4.5-preview	92.63	89.40	-3.23
anthropic/claude-3.5-sonnet	91.24	89.40	-1.84
openai/gpt-4o	90.74	87.10	-3.64
dziner-qwen-2.5-72b	90.32	86.18	-4.14
qwen/qwen3-next-80b-a3b-instruct	90.32	89.40	-0.92
perplexity/sonar-pro	90.32	88.02	-2.30
deepseek/deepseek-v3.1-terminus	89.86	90.78	+0.92
qwen/qwen-plus	89.86	89.40	-0.46
qwen/qwen3-next-80b-a3b-thinking	89.86	87.10	-2.76
deepseek/deepseek-chat	89.40	90.32	+0.92
qwen/qwen-max	89.40	89.40	+0.00
o1	89.40	88.94	-0.46
anthropic/claude-3-opus	88.94	88.94	+0.00
openai/o1-mini	88.02	88.02	+0.00
meta-llama/llama-3.1-405b-instruct	87.56	84.33	-3.23
qwen/qwen-2.5-72b-instruct	87.56	85.71	-1.85
mistralai/mistral-large	86.18	86.18	+0.00
amazon/nova-pro-v1	86.11	86.64	+0.53
gpt-4-turbo	85.25	85.71	+0.46
meta-llama/llama-3-70b-instruct	84.79	82.95	-1.84
meta-llama/llama-3.1-70b-instruct	84.79	85.19	+0.40
dziner-qwen-2.5-coder-32b	83.87	77.42	-6.45
openai/gpt-4-o314	83.41	82.49	-0.92
gpt-4-turbo-preview	83.41	84.79	+1.38
amazon/nova-lite-v1	82.03	85.71	+3.68
dziner-qwen-2.5-7b	81.57	79.26	-2.31
gpt-4	81.57	82.49	+0.92
openai/gpt-4o-mini	81.11	81.11	+0.00
openrouter/auto	81.11	81.57	+0.46
qwen/qwen-2.5-7b-instruct	79.72	78.34	-1.38
google/gemma-2-27b-it	79.26	79.72	+0.46
anthropic/claude-3.5-haiku	77.57	85.92	+8.35
mistralai/mixtral-8x22b-instruct	76.81	83.89	+7.08
mistralai/mistral-7b-instruct	75.35	80.65	+5.30
google/gemma-2-9b-it	75.12	81.57	+6.45
amazon/nova-micro-v1	74.65	80.65	+6.00
mistralai/mistral-small	74.65	83.41	+8.76
anthropic/claude-3-haiku	74.04	83.33	+9.29
openai/gpt-3.5-turbo-16k	72.60	75.85	+3.25
mistralai/mixtral-8x7b-instruct	72.33	77.14	+4.81
meta-llama/llama-3-8b-instruct	71.89	75.58	+3.69
mistralai/pixtral-12b	71.83	77.88	+6.05
openai/gpt-3.5-turbo	70.67	76.33	+5.66
meta-llama/llama-3.1-8b-instruct	69.12	78.34	+9.22
llava-v1.6-34b	66.82	78.34	+11.52
lmsys-lab/llava-onevision-qwen2-7b-si	66.36	75.12	+8.76
lmsys-lab/llava-onevision-qwen2-7b-ov-chat	65.90	76.04	+10.14
lmsys-lab/llava-onevision-qwen2-7b-ov	65.44	74.19	+8.75
meta-llama/llama-3.2-3b-instruct	64.98	65.44	+0.46
arcee-ai/afm-4.5b	62.21	67.28	+5.07
mistralai/mistral-7b-instruct-v0.1	59.50	62.44	+2.94
perplexity/sonar	59.24	67.14	+7.90
undi95/remm-slerp-l2-13b	57.08	65.12	+8.04
llamat-3-chat	57.14	31.80	-25.34
alibaba/tongyi-deepresearch-30b-a3b	55.76	86.64	+30.88
gryphe/mythomax-l2-13b	53.77	66.51	+12.74
llava-v1.6-mistral-7b	52.99	64.06	+11.07
llamat-2-chat	50.69	16.13	-34.56
lmsys-lab/llava-onevision-qwen2-0.5b-ov	47.47	54.38	+6.91
llava-v1.5-13b	46.54	48.39	+1.85
lmsys-lab/llava-onevision-qwen2-0.5b-si	46.08	53.91	+7.83
qwen/qwen3-coder-flash	43.46	85.71	+42.25
qwen/qwen3-coder-plus	22.99	88.94	+65.95
honeybee-13b	22.12	21.20	-0.92
qwen/qwen-2.5-coder-32b-instruct	21.03	30.77	+9.74
honeybee-7b	19.35	17.51	-1.84
llava-v1.5-7b	17.97	28.57	+10.60
llamat-2	16.59	19.82	+3.23

Table 6 LLM-based quality ratings (0–10) for 217 helper pairs. Scores are means across questions.

Metric	AI helper	Human helper	Δ
Accuracy	7.43	9.25	+1.82
Clarity	7.53	8.91	+1.38
Completeness	7.40	9.20	+1.81
Reliability	7.30	9.17	+1.87
Overall mean	7.41	9.13	+1.72

phase identification in multiphase inorganic compounds us-

ing synthetic xrd powder patterns. *Nature communications*, 11(1):86, 2020.

- 30 Nathan J Szymanski, Christopher J Bartel, Yan Zeng, Mouhamad Diallo, Haegyem Kim, and Gerbrand Ceder. Adaptively driven x-ray diffraction guided by machine learning for autonomous phase identification. *npj Computational Materials*, 9(1):31, 2023.
- 31 Felix A Faber, Luke Hutchison, Bing Huang, Justin Gilmer, Samuel S Schoenholz, George E Dahl, Oriol Vinyals, Steven Kearnes, Patrick F Riley, and O Anatole Von Lilienfeld. Prediction errors of molecular machine learning models lower than hybrid dft error. *Journal of chemical theory and computation*, 13(11):5255–5264, 2017.
- 32 Vasile-Adrian Surdu and Romuald György. X-ray diffraction data analysis by machine learning methods—a review. *Applied Sciences*, 13(17):9992, 2023.
- 33 Byung Do Lee, Jin-Woong Lee, Junuk Ahn, Seonghwan Kim, Woon Bae Park, and Kee-Sun Sohn. A deep learning approach to powder x-ray diffraction pattern analysis: Addressing generalizability and perturbation issues simultaneously. *Advanced Intelligent Systems*, 5(9):2300140, 2023.
- 34 Longlong Wu, Shinjae Yoo, Ana F Suzana, Tadesse A Assefa, Jiecheng Diao, Ross J Harder, Wonsuk Cha, and Ian K Robinson. Three-dimensional coherent x-ray diffraction imaging via deep convolutional neural networks. *npj Computational Materials*, 7(1):175, 2021.
- 35 Naomi E Omori, Antonia D Bobitan, Antonis Vamvakeros, Andrew M Beale, and Simon DM Jacques. Recent developments in x-ray diffraction/scattering computed tomography for materials science. *Philosophical Transactions of the Royal Society A*, 381(2259):20220350, 2023.
- 36 Emigdio Chávez-Angel, Martin Børstad Eriksen, Alejandro Castro-Alvarez, Jose H Garcia, Marc Botifoll, Oscar Avalos-Ovando, Jordi Arbiol, and Aitor Mugarza. Applied artificial intelligence in materials science and material design. *Advanced Intelligent Systems*, page 2400986, 2025.
- 37 Yiheng Liu, Tianle Han, Siyuan Ma, Jiayue Zhang, Yuanyuan Yang, Jiaming Tian, Hao He, Antong Li, Mengshen He, Zhengliang Liu, et al. Summary of chatgpt-related research and perspective towards the future of large language models. *Meta-radiology*, 1(2):100017, 2023.
- 38 Muhammad Usman Hadi, Rizwan Qureshi, Abbas Shah, Muhammad Irfan, Anas Zafar, Muhammad Bilal Shaikh, Naveed Akhtar, Jia Wu, Seyedali Mirjalili, et al. Large language models: a comprehensive survey of its applications, challenges, limitations, and future prospects. *Authorea Preprints*, 1:1–26, 2023.
- 39 Matthew Dahl, Varun Magesh, Mirac Suzgun, and Daniel E Ho. Large legal fictions: Profiling legal hallucinations in large language models. *Journal of Legal Analysis*, 16(1):64–93, 2024.
- 40 Yuchen Zhuang, Yue Yu, Kuan Wang, Haotian Sun, and Chao Zhang. Toolqa: A dataset for llm question answering with external tools. *Advances in Neural Information Processing Systems*, 36:50117–50143, 2023.

Table 7 Direct comparison of performance gains between AI-generated supporting materials with and without expert review.

Model	AI-Generated Δ (%)	Expert-Reviewed Δ (%)	Difference
openai/gpt-5	-1.84	-3.68	-1.84
x-ai/grok-4-fast	-0.92	-5.78	-4.86
openai/gpt-5-codex	-1.84	-4.14	-2.30
google/gemini-2.5-pro	-6.91	-2.76	+4.15
o3-mini	-4.15	-3.69	+0.46
meituan/longcat-flash-chat	-2.77	-3.23	-0.46
gpt-4.5-preview	-2.31	-3.23	-0.92
anthropic/claude-3.5-sonnet	-1.84	-1.84	+0.00
openai/gpt-4o	-3.18	-3.64	-0.46
dziner-qwen-2.5-72b	-3.22	-4.14	-0.92
qwen/qwen3-next-80b-a3b-instruct	-0.92	-0.92	+0.00
perplexity/sonar-pro	+0.00	-2.30	-2.30
deepseek/deepseek-v3.1-terminus	+0.92	+0.92	+0.00
qwen/qwen-plus	+0.92	-0.46	-1.38
qwen/qwen3-next-80b-a3b-thinking	-2.76	-2.76	+0.00
deepseek/deepseek-chat	+1.84	+0.92	-0.92
qwen/qwen-max	-1.38	+0.00	+1.38
o1	-1.38	-0.46	+0.92
anthropic/claude-3-opus	-0.92	+0.00	+0.92
openai/o1-mini	+0.46	+0.00	-0.46
meta-llama/llama-3.1-405b-instruct	-4.61	-3.23	+1.38
qwen/qwen-2.5-72b-instruct	-1.38	-1.85	-0.47
mistralai/mistral-large	-2.31	+0.00	+2.31
amazon/nova-pro-v1	+0.53	+0.53	+0.00
gpt-4-turbo	+0.46	+0.46	+0.00
meta-llama/llama-3-70b-instruct	-4.14	-1.84	+2.30
meta-llama/llama-3.1-70b-instruct	-1.38	+0.40	+1.78
dziner-qwen-2.5-coder-32b	+0.92	-6.45	-7.37
openai/gpt-4-0314	-5.99	-0.92	+5.07
gpt-4-turbo-preview	-0.92	+1.38	+2.30
amazon/nova-lite-v1	+2.76	+3.68	+0.92
dziner-qwen-2.5-7b	-2.31	-2.31	+0.00
gpt-4	+0.46	+0.92	+0.46
openai/gpt-4o-mini	+0.92	+0.00	-0.92
openrouter/auto	+0.46	+0.46	+0.00
qwen/qwen-2.5-7b-instruct	-4.60	-1.38	+3.22
google/gemma-2-27b-it	-0.46	+0.46	+0.92
anthropic/claude-3.5-haiku	+10.45	+8.35	-2.10
mistralai/mixtral-8x22b-instruct	+3.28	+7.08	+3.80
mistralai/mistral-7b-instruct	+2.07	+5.30	+3.23
google/gemma-2-9b-it	+2.30	+6.45	+4.15
amazon/nova-micro-v1	+4.61	+6.00	+1.39
mistralai/mistral-small	+4.61	+8.76	+4.15
anthropic/claude-3-haiku	+8.45	+9.29	+0.84
openai/gpt-3.5-turbo-16k	-1.59	+3.25	+4.84
mistralai/mixtral-8x7b-instruct	+3.63	+4.81	+1.18
meta-llama/llama-3-8b-instruct	+1.38	+3.69	+2.31
mistralai/pixtral-12b	+3.75	+6.05	+2.30
openai/gpt-3.5-turbo	+0.83	+5.66	+4.83
meta-llama/llama-3.1-8b-instruct	+6.00	+9.22	+3.22
llava-v1.6-34b	+5.99	+11.52	+5.53
lmms-lab/llava-onevision-qwen2-7b-si	+5.53	+8.76	+3.23
lmms-lab/llava-onevision-qwen2-7b-ov-chat	+6.45	+10.14	+3.69
lmms-lab/llava-onevision-qwen2-7b-ov	+5.99	+8.75	+2.76
meta-llama/llama-3.2-3b-instruct	-2.31	+0.46	+2.77
arcee-ai/afm-4.5b	+2.31	+5.07	+2.76
mistralai/mistral-7b-instruct-v0.1	-5.47	+2.94	+8.41
perplexity/sonar	+9.60	+7.90	-1.70
undi95/remm-slerp-l2-13b	+4.42	+8.04	+3.62
llamat-3-chat	-26.73	-25.34	+1.39
alibaba/tongyi-deepresearch-30b-a3b	+24.42	+30.88	+6.46
gryphe/mythomax-l2-13b	+7.91	+12.74	+4.83
llava-v1.6-mistral-7b	+5.54	+11.07	+5.53
llamat-2-chat	-29.56	-34.56	-5.00
lmms-lab/llava-onevision-qwen2-0.5b-ov	+3.68	+6.91	+3.23
llava-v1.5-13b	-2.30	+1.85	+4.15
lmms-lab/llava-onevision-qwen2-0.5b-si	+5.07	+7.83	+2.76
qwen/qwen3-coder-flash	+40.87	+42.25	+1.38
qwen/qwen3-coder-plus	+65.95	+65.95	+0.00
honeybee-13b	+0.92	-0.92	-1.84
qwen/qwen-2.5-coder-32b-instruct	+5.98	+9.74	+3.76
honeybee-7b	+3.69	-1.84	-5.53
llava-v1.5-7b	+5.99	+10.60	+4.61
llamat-2	+3.23	+3.23	+0.00

Table 8 Selected subtask-level accuracy (%) for LLaVA-onevision-QWEN2-7B-ov, comparing closed-book mode vs. open-book mode with expert-reviewed materials. Some subtasks have fewer questions, so a single item shifts accuracy considerably.

Subtask	Closed-book mode	Open-book mode	Improvement
<i>Large Gains</i>			
Atomic Spacing	66.7	100.0	+33.3
Coordination Numbers	20.0	60.0	+40.0
Crystal Structure	0.0	100.0	+100.0
Laue Patterns	0.0	100.0	+100.0
Metal Structures	0.0	100.0	+100.0
Powder Diffraction	0.0	100.0	+100.0
Structure Factors	60.0	85.0	+25.0
<i>Little / No Improvement</i>			
Bragg's Law	0.0	0.0	+0.0
Calculation Methods	0.0	0.0	+0.0
Diffraction Limitations	0.0	0.0	+0.0
<i>Performance Drops</i>			
Complex Mathematics	100.0	50.0	-50.0
Wave Scattering	100.0	0.0	-100.0

- 41 Ehsan Kamalloo, Nouha Dziri, Charles LA Clarke, and Davood Rafiei. Evaluating open-domain question answering in the era of large language models. *arXiv preprint arXiv:2305.06984*, 2023.
- 42 Zhiyuan Chen, Yaning Li, and Kairui Wang. Optimizing reasoning abilities in large language models: A step-by-step approach. *Authorea Preprints*, 2024.
- 43 Nisarg Patel, Mohith Kulkarni, Mihir Parmar, Aashna Budhiraja, Mutsumi Nakamura, Neeraj Varshney, and Chitta Baral. Multi-logieval: Towards evaluating multi-step logical reasoning ability of large language models. *arXiv preprint arXiv:2406.17169*, 2024.
- 44 Mohd Zaki, NM Anoop Krishnan, et al. Mascqa: investigating materials science knowledge of large language models. *Digital Discovery*, 3(2):313–327, 2024.
- 45 Lukas Schulze Balhorn, Jana M Weber, Stefan Buijsman, Julian R Hildebrandt, Martina Ziefle, and Artur M Schweidtmann. What does chatgpt know about natural science and engineering? *arXiv preprint arXiv:2309.10048*, 2023.
- 46 Adrian Mirza, Nawaf Alampara, Sreekanth Kunchapu, Martiño Ríos-García, Benedict Emoekabu, Aswanth Krishnan, Tanya Gupta, Mara Schilling-Wilhelmi, Maçjonathan Okereke, Anagha Aneesh, et al. Are large language models superhuman chemists? *arXiv preprint arXiv:2404.01475*, 2024.
- 47 Kamal Choudhary. Microscopygpt: Generating atomic-structure captions from microscopy images of 2d materials with vision-language transformers. *The Journal of Physical Chemistry Letters*, 16:7028–7035, 2025.
- 48 Andre Niyongabo Rubungo, Craig Arnold, Barry P Rand, and Adji Bouso Dieng. Llm-prop: Predicting physical and electronic properties of crystalline solids from their text descriptions. *arXiv preprint arXiv:2310.14029*, 2023.
- 49 Chen Qian, Huayi Tang, Zhirui Yang, Hong Liang, and Yong Liu. Can large language models empower molecular property prediction? *arXiv preprint arXiv:2307.07443*, 2023.
- 50 Youjia Li, Vishu Gupta, Muhammed Nur Talha Kilic, Kamal Choudhary, Daniel Wines, Wei-keng Liao, Alok Choudhary, and Ankit Agrawal. Hybrid-llm-gnn: integrating large language models and graph neural networks for enhanced materials property prediction. *Digital Discovery*, 2025.
- 51 Yuan Chiang, Chia-Hong Chou, and Janosh Riebesell. LLaMP: Large language model made powerful for high-fidelity materials knowledge retrieval and distillation. *arXiv preprint arXiv:2401.17244*, 2024.
- 52 Tanishq Gupta, Mohd Zaki, N. M. Anoop Krishnan, and Mausam. Matscibert: A materials domain language model for text mining and information extraction. *npj Computational Materials*, 8(1):102, 2022.
- 53 Songlin Yu, Nian Ran, and Jianjun Liu. Large-language models: The game-changers for materials science research. *Artificial Intelligence Chemistry*, 2(2):100076, 2024.

- 54 Yuang Shi, Nakul Rampal, Chengbin Zhao, Dongrong Joe Fu, Christian Borgs, Jennifer T Chayes, and Omar M Yaghi. Comparison of llms in extracting synthesis conditions and generating q&a datasets for metal-organic frameworks. *Digital Discovery*, 2025.
- 55 Hongchen Wang, Kangming Li, Scott Ramsay, Yao Fehlis, Edward Kim, and Jason Hatrick-Simpers. Evaluating the performance and robustness of llms in materials science q&a and property predictions. *Digital Discovery*, 2025.
- 56 Luis M. Antunes, Keith T. Butler, and Ricardo Grau-Crespo. Crystal structure generation with autoregressive large language modeling. *Nature Communications*, 15:10570, 2024.
- 57 Frederik Lizak Johansen, Ulrik Friis-Jensen, Erik Bjørnager Dam, Kirsten Marie Ørnsbjerg Jensen, Rocío Mercado, and Raghavendra Selvan. deCIFer: Crystal structure prediction from powder diffraction data using autoregressive language models. *arXiv preprint arXiv:2502.02189*, 2025.
- 58 Kamal Choudhary. DiffraCtGPT: Atomic structure determination from x-ray diffraction patterns using a generative pre-trained transformer. *The Journal of Physical Chemistry Letters*, 16(8):2110–2119, 2025.
- 59 Kamal Choudhary. AtomGPT: Atomistic generative pre-trained transformer for forward and inverse materials design. *The Journal of Physical Chemistry Letters*, 15(27):6909–6917, 2024.
- 60 Edward J Hu, Yelong Shen, Phillip Wallis, Zeyuan Allen-Zhu, Yuanzhi Li, Shean Wang, Lu Wang, and Weizhu Chen. LoRA: Low-rank adaptation of large language models. In *International Conference on Learning Representations*, 2022.
- 61 OpenAI. Introducing gpt-5. OpenAI Blog, August 2025. Released August 7, 2025.
- 62 OpenAI. Introducing upgrades to codex: Gpt-5-codex. OpenAI Blog, September 2025. Released September 23, 2025; optimized version of GPT-5 for agentic coding.
- 63 OpenAI. OpenAI o3-mini system card. OpenAI Technical Report, January 2025. Released January 31, 2025.
- 64 OpenAI. OpenAI o1 system card, December 2024. System card for o1 and o1-mini models.
- 65 OpenAI. Introducing gpt-4.5. OpenAI Blog, February 2025. Code-named Orion; released February 27, 2025; OpenAI’s largest pre-trained model.
- 66 OpenAI. Gpt-4o system card, October 2024. Omnimodal model accepting text, audio, image, and video inputs; includes GPT-4o-mini.
- 67 OpenAI. New models and developer products announced at devday. OpenAI Blog, November 2023. GPT-4 Turbo with 128K context window; gpt-4-1106-preview and subsequent versions.
- 68 OpenAI. Gpt-4 technical report, March 2023. Multimodal model accepting image and text inputs.
- 69 OpenAI. Introducing chatgpt and whisper apis. OpenAI Blog, March 2023. GPT-3.5-turbo (gpt-3.5-turbo-0301) released March 1, 2023; powers ChatGPT.
- 70 OpenAI. Gpt-3.5 turbo fine-tuning and api updates. OpenAI Blog, June 2023. GPT-3.5-turbo-16k with extended 16K context window announced June 13, 2023.
- 71 Anthropic. The Claude 3 model family: Opus, Sonnet, Haiku. Technical report, Anthropic, March 2024. Model Card.
- 72 Anthropic. Claude 3.5 Sonnet model card addendum. Technical report, Anthropic, June 2024. Model Card Addendum.
- 73 Anthropic. Model card addendum: Claude 3.5 Haiku and upgraded Claude 3.5 Sonnet. Technical report, Anthropic, October 2024. Model Card Addendum.
- 74 Llama Team. The llama 3 herd of models. *arXiv preprint arXiv:2407.21783*, July 2024. Version 3, revised November 23, 2024. Covers LLaMA-3-8B/70B-instruct and LLaMA-3.1-8B/70B/405B-instruct.
- 75 Meta AI. Llama 3.2: Revolutionizing edge ai and vision with open, customizable models. Meta AI Blog, September 2024. Announced at Meta Connect 2024. Covers LLaMA-3.2-1B/3B-instruct.
- 76 An Yang, Anfeng Li, Baosong Yang, Beichen Zhang, Binyuan Hui, Bo Zheng, Bowen Yu, Chang Gao, Chengen Huang, Chenxu Lv, Chujie Zheng, Dayiheng Liu, Fan Zhou, Fei Huang, Feng Hu, Hao Ge, Haoran Wei, Huan Lin, Jialong Tang, Jian Yang, Jianhong Tu, Jianwei Zhang, Jianxin Yang, Jiayi Yang, Jing Zhou, Jingren Zhou, Junyang Lin, Kai Dang, Keqin Bao, Kexin Yang, Le Yu, Lianghao Deng, Mei Li, Mingfeng Xue, Mingze Li, Pei Zhang, Peng Wang, Qin Zhu, Rui Men, Ruize Gao, Shixuan Liu, Shuang Luo, Tianhao Li, Tianyi Tang, Wenbiao Yin, Xingzhang Ren, Xinyu Wang, Xinyu Zhang, Xuancheng Ren, Yang Fan, Yang Su, Yichang Zhang, Yinger Zhang, Yu Wan, Yuqiong Liu, Zekun Wang, Zeyu Cui, Zhenru Zhang, Zhipeng Zhou, and Zihan Qiu. Qwen3 technical report. *arXiv preprint arXiv:2505.09388*, May 2025.
- 77 Qwen, An Yang, Baosong Yang, Beichen Zhang, Binyuan Hui, Bo Zheng, Bowen Yu, Chengyuan Li, Dayiheng Liu, Fei Huang, Haoran Wei, Huan Lin, Jian Yang, Jianhong Tu, Jianwei Zhang, Jianxin Yang, Jiayi Yang, Jingren Zhou, Junyang Lin, Kai Dang, Keming Lu, Keqin Bao, Kexin Yang, Le Yu, Mei Li, Mingfeng Xue, Pei Zhang, Qin Zhu, Rui Men, Runji Lin, Tianhao Li, Tianyi Tang, Tingyu Xia, Xingzhang Ren, Xuancheng Ren, Yang Fan, Yang Su, Yichang Zhang, Yu Wan, Yuqiong Liu, Zeyu Cui, Zhenru Zhang, and Zihan Qiu. Qwen2.5 technical report. *arXiv preprint arXiv:2412.15115*, December 2024.
- 78 Qwen Team. Qwen3-coder: The code version of qwen3. <https://github.com/QwenLM/Qwen3-Coder>, 2025. Based on Qwen3 Technical Report, arXiv:2505.09388.
- 79 Binyuan Hui, Jian Yang, Zeyu Cui, Jiayi Yang, Dayiheng Liu, Lei Zhang, Tianyu Liu, Jiajun Zhang, Bowen Yu, Kai Dang, An Yang, Rui Rong, Yichang Xue, Jingren Fu, Jingren Ma, and Junyang Lin. Qwen2.5-coder technical report. *arXiv preprint arXiv:2409.12186*, September 2024.
- 80 Tongyi DeepResearch Team and Tongyi Lab. Tongyi-deepresearch: An agentic large language model for deep information-seeking tasks. <https://github.com/Alibaba-NLP/DeepResearch>, 2025. 30B total parameters,

- 3B activated per token.
- 81 Mistral AI Team. Au large: Mistral large. Mistral AI Blog, February 2024. 123B parameters, 32K context window, available on Azure and La Plateforme.
 - 82 Mistral AI Team. Mistral small: Optimized model for low latency workloads. Mistral AI Blog, February 2024. Released alongside Mistral Large, optimized for latency and cost.
 - 83 Albert Q. Jiang, Alexandre Sablayrolles, Arthur Mensch, Chris Bamford, Devendra Singh Chaplot, Diego de las Casas, Florian Bressand, Gianna Lengyel, Guillaume Lample, Lucile Saulnier, L lio Renard Lavaud, Marie-Anne Lachaux, Pierre Stock, Teven Le Scao, Thibaut Lavril, Thomas Wang, Timoth e Lacroix, and William El Sayed. Mistral 7b. *arXiv preprint arXiv:2310.06825*, October 2023. Apache 2.0 license.
 - 84 Albert Q. Jiang, Alexandre Sablayrolles, Antoine Roux, Arthur Mensch, Blanche Savary, Chris Bamford, Devendra Singh Chaplot, Diego de las Casas, Emma Bou Hanna, Florian Bressand, Gianna Lengyel, Guillaume Bour, Guillaume Lample, L lio Renard Lavaud, Lucile Saulnier, Marie-Anne Lachaux, Pierre Stock, Sandeep Subramanian, Sophia Yang, Szymon Antoniak, Teven Le Scao, Th ophile Gervet, Thibaut Lavril, Thomas Wang, Timoth e Lacroix, and William El Sayed. Mixtral of experts. *arXiv preprint arXiv:2401.04088*, January 2024. Apache 2.0 license.
 - 85 Mistral AI Team. Cheaper, better, faster, stronger: Mixtral 8x22b. Mistral AI Blog, April 2024. 141B parameters with 39B active, Apache 2.0 license.
 - 86 Praveesh Agrawal, Szymon Antoniak, Emma Bou Hanna, Baptiste Bout, Devendra Chaplot, Jessica Chudnovsky, Diogo Costa, Baudouin De Monicault, Saurabh Garg, Theophile Gervet, Soham Ghosh, Am lie H liou, Paul Jacob, Albert Q. Jiang, Kartik Khandelwal, Timoth e Lacroix, Guillaume Lample, Diego Las Casas, Thibaut Lavril, Teven Le Scao, Andy Lo, William Marshall, Louis Martin, Arthur Mensch, Pavankumar Muddireddy, Valera Nemychnikova, Marie Pellat, Patrick Von Platen, Nikhil Raghuraman, Baptiste Rozi re, Alexandre Sablayrolles, Lucile Saulnier, Romain Sauvestre, Wendy Shang, Roman Soletskyi, Lawrence Stewart, Pierre Stock, Joachim Studnia, Sandeep Subramanian, Sagar Vaze, Thomas Wang, and Sophia Yang. Pixtral 12b. *arXiv preprint arXiv:2410.07073*, October 2024. Apache 2.0 license, 128K context window.
 - 87 DeepSeek-AI. Deepseek-v3 technical report, 2024.
 - 88 Gemini Team. Gemini 2.5: Pushing the frontier with advanced reasoning, multimodality, long context, and next generation agentic capabilities. Technical report, Google DeepMind, 2025. Technical Report.
 - 89 Gemma Team: Morgane Riviere and Shreya Pathak and Pier Giuseppe Sessa and Cassidy Hardin and Surya Bhupatiraju and L onard Hussenot and Thomas Mesnard and Bobak Shahriari and others. Gemma 2: Improving open language models at a practical size, 2024.
 - 90 Amazon Artificial General Intelligence. The Amazon Nova family of models: Technical report and model card. Technical report, Amazon, December 2024. Models: Amazon Nova Pro, Amazon Nova Lite, Amazon Nova Micro.
 - 91 xAI. Grok 4 fast model card. Technical report, xAI, September 2025. Multimodal reasoning model with 2M token context window.
 - 92 Haotian Liu, Chunyuan Li, Yuheng Li, Bo Li, Yuanhan Zhang, Sheng Shen, and Yong Jae Lee. Llava-next: Improved reasoning, ocr, and world knowledge. <https://llava-v1.github.io/blog/2024-01-30-llava-next/>, January 2024.
 - 93 Haotian Liu, Chunyuan Li, Yuheng Li, and Yong Jae Lee. Improved baselines with visual instruction tuning, 2023.
 - 94 Bo Li, Yuanhan Zhang, Dong Guo, Renrui Zhang, Feng Li, Hao Zhang, Kaichen Zhang, Yanwei Li, Ziwei Liu, and Chunyuan Li. Llava-onevision: Easy visual task transfer, 2024.
 - 95 Vaibhav Mishra, Somaditya Singh, Dhruv Ahlawat, Mohd Zaki, Vaibhav Bihani, Hargun Singh Grover, Biswajit Mishra, Santiago Miret, Mausam, and N. M. Anoop Krishnan. Foundational large language models for materials research. *arXiv preprint arXiv:2412.09560*, 2024.
 - 96 Mehrad Ansari, Joshua Watchorn, Cameron E Brown, and James S Brown. dziner: Rational inverse design of materials with ai agents. In *AI for Accelerated Materials Design-NeurIPS 2024*, 2024.
 - 97 Perplexity AI. Sonar pro: Advanced search model with enhanced results. <https://docs.perplexity.ai/getting-started/models/models/sonar-pro>, January 2025. Context window: 200,000 tokens. Enhanced search capabilities with 2x more citations.
 - 98 Perplexity AI. Meet new sonar: A blazing fast model optimized for perplexity search. <https://www.perplexity.ai/hub/blog/meet-new-sonar>, February 2025. Built on Llama 3.3 70B. Context window: 127,000 tokens.
 - 99 Meituan LongCat Team, Bayan, Bei Li, Bingye Lei, et al. LongCat-Flash technical report. *arXiv preprint arXiv:2509.01322*, 2025. 560B total parameters with 18.6B-31.3B activated per token.
 - 100 Arcee.ai. AFM-4.5B: A 4.5 billion parameter instruction-tuned foundation model. <https://huggingface.co/arcee-ai/AFM-4.5B>, 2025. HuggingFace model card. Trained on 8 trillion tokens (6.5T pretraining + 1.5T mid-training). Apache-2.0 license.
 - 101 Undi95. ReMM-SLERP-L2-13B: A recreation of mythomax with updated models. <https://huggingface.co/Undi95/ReMM-SLERP-L2-13B>, 2023. HuggingFace model card. Re:MythoMax (ReMM) is a recreation trial of the original MythoMax-L2-B13 with updated models using SLERP merging technique.
 - 102 Gryphe. MythoMax-L2-13b: An improved variant of mythomix. <https://huggingface.co/Gryphe/MythoMax-L2-13b>, 2023. HuggingFace model card. A merge of MythoLogic-L2 and Huginn using a highly experimental tensor type merge technique.
 - 103 Junbum Cha, Wooyoung Kang, Jonghwan Mun, and Byungseok Roh. Honeybee: Locality-enhanced projector for

- multimodal llm, December 2023.
- 104 OpenRouter. OpenRouter Auto Router: Dynamic model selection powered by Not Diamond. <https://openrouter.ai/openrouter/auto>, November 2023. Model routing service created November 8, 2023. Routes prompts to optimal models using Not Diamond meta-model.
- 105 Siddharth M. Narayanan, James D. Braza, Ryan-Rhys Griffiths, Albert Bou, Geemi P. Wellawatte, Mayk Caldas Ramos, Ludovico Mitchener, Samuel G. Rodrigues, and Andrew D. White. Training a scientific reasoning model for chemistry. *arXiv preprint arXiv:2506.17238*, June 2025. 24B parameter reasoning model for chemistry trained with reinforcement learning. Based on Mistral-Small-24B-Instruct-2501.
- 106 Aaron Meurer, Christopher P Smith, Mateusz Paprocki, Ondřej Čertík, Sergey B Kirpichev, Matthew Rocklin, AMiT Kumar, Sergiu Ivanov, Jason K Moore, Sartaj Singh, et al. Sympy: Symbolic computing in python. *PeerJ Computer Science*, 3:e103, 2017.
- 107 Wolfram Research. Wolfram alpha. <https://www.wolframalpha.com>, 2009.
- 108 Brian H Toby and Robert B Von Dreele. Gsas-ii: The genesis of a modern open-source all purpose crystallography software package. *Journal of Applied Crystallography*, 46(2):544–549, 2013.
- 109 Colin F Macrae, Ioana Sovago, Stephen J Cottrell, Peter TA Galek, Patrick McCabe, Elna Pidcock, Michael Platings, Gregory P Shields, John S Stevens, Matthew Towler, et al. Mercury 4.0: From visualization to analysis, design and prediction. *Journal of Applied Crystallography*, 53(1):226–235, 2020.